

Nora Rønningen

Experimental investigation of nutrient competition between starved *Saccharina latissima* and phytoplankton.

Master's thesis in Ocean Resources

Supervisor: Yngvar Olsen (IBI)

Co-supervisor: Ana Borrero (Seaweed Solutions AS), Siv Anina Etter (IBI) and Sturla Haltbakk (IBI)

May 2023

Nora Rønningen

**Experimental investigation of nutrient
competition between starved
Saccharina latissima and phytoplankton.**

Master's thesis in Ocean Resources

Supervisor: Yngvar Olsen (IBI)

Co-supervisor: Ana Borrero (Seaweed Solutions AS), Siv Anina Etter
(IBI) and Sturla Haltbakk (IBI)

May 2023

Norwegian University of Science and Technology

Faculty of Natural Sciences

Department of Biology



Norwegian University of
Science and Technology

Acknowledgements

This master thesis was completed at the Department of Biology at NTNU Trondheim in collaboration with Seaweed Solutions (SES). The experiment and lab work were conducted at Trondheim biological station (TBS) from January 2022 to February 2023. My main supervisor was Yngvar Olsen (NTNU), and my co-supervisors were Ana Borrero (SES), Siv Anina Etter at NTNU and Sturla Haltbakk (NTNU).

Firstly, I would like to express my gratitude to my main supervisor Yngvar Olsen for constructing this thesis and giving me the opportunity to work with seaweed and collaborate with Seaweed solutions. Thank you for your enthusiasm, guidance, feedback and all the time and thought put into this project. Secondly, to my co-supervisors, Ana Borrero for the feedback and the support I have gotten when I have needed it. To Siv Anina Etter for all the help and guidance during my lab work and calculations and for supervising all the analysis, and to Sturla Haltbakk for designing the experimental set up, and for all the hours we spent setting up the experiment during the cold rainy winter days.

I would also like to thank SES for providing me the seeded lines of *Saccharina latissima* I used in this project, and to Elin Njåstad for supervising me during my first sampling day.

I'm also grateful to the staff and students at TBS that created a warm and welcoming work environment. I would like to give a special thanks to Thea Svendsen, Gitte Krohn-Pettersen and Martin Molberg Overrein for all support and fun we had sitting late nights at TBS and swimming every Monday. I would also like to express my sincerest gratitude to NJORD and all my fellow students at Ocean Resources for creating a social and memorable time.

Finally, I would like to thank my family and friends that have supported me and been there for me during the ups and downs.

Trondheim, May 2023

Nora Rønningen

Abstract

Large scale cultivation of seaweed is a sustainable industry that can be used as food for human consumption and other products. Seaweed is an important source for the food security of the growing human population. To upscale the production of seaweed, knowledge about the nutrient uptake, growth kinetics and interactions with the ecosystem are essential. Nutrients are key factors that limits growth of seaweed. During the winter the nutrient concentration in seawater is high due to mixing of the water column. However, when light availability and temperature increases during the spring, nutrients become the limiting factor, due to stratification of the water and phytoplankton bloom. Phytoplankton and seaweed compete for the same resources for growth and other metabolic processes. The potential interaction between phytoplankton and seaweed have raised a concern. Recent publications have described potential impacts to the phytoplankton communities derived by a large scale of seaweed cultivation.

Based on this, the aim of this thesis was to investigate if there is a competition of inorganic nutrients between phytoplankton communities and *Saccharina latissima*, and if a fertilization treatment could increase the competitive ability, growth and nutritional state. To do so, an experiment was carried comparing one control (CTL) treatment that were undisturbed, and one treatment where the sporophytes (FER) got a boost of nutrients for 24 and 48 hours with inorganic nitrate (NO_3^-) and phosphate (PO_4^{3-}) in an external tank. Nutrient composition, net uptake, and growth of the two treatments were examined and compared with water samples that showed the nutritional status of phytoplankton.

The results showed that the phytoplankton community had maximum growth and high biomass during the whole experiment and was not negatively affected by *S. latissima*. By using the Droop-model a correlation between specific growth rate and the internal nutrient content in *S. latissima* were found, it also showed that the young sporophytes in the winter period had the highest internal nutrient content (Q_m) that lead to maximum growth (μ_{\max}). The high nutrient content in the winter period, suggested that the sporophytes have higher storage capacity in the winter and uses it for growth when the ambient nutrients decrease. The results also showed that there was a significant difference in growth, health and nutrient composition between the FER and CTL sporophytes in June. The CTL sporophytes showed decreasing nutrient content, chlorophyll *a* level, growth, negative net uptake, and tissue with low or no photosynthetic activity. The FER sporophytes on the other hand showed increased values of nutrient content, Chl *a*, growth, net uptake of nutrients and photosynthetic efficiency. By comparing the phytoplankton, CTL and FER sporophytes, the results suggested that there is a competition between *S. latissima* and phytoplankton when it comes to taking up nutrients and that fertilization treatment can increase the competitive ability of nutrient uptake.

Sammendrag

Kultivering av makroalger er en bærekraftig industri med stort potensiale for å produsere mat og andre produkter. Makroalger kan derfor være en viktig kilde til å øke matsikkerheten til den økende globale befolkningen. Kunnskap om næringsopptak, vekst og interaksjoner makroalgene har med økosystemet er viktig for å kunne øke makroalgeproduksjonen. Næringsstoffer er en av nøkkelfaktorene som begrenser vekst hos makroalger. På vinteren er næringskonsentrasjonen i sjøvann høy på grunn av liten lagdeling og lite blanding av vannmasser i vannsøyla. Ved økt lys og temperatur i løpet av våren blir næringsstoff den begrensende faktoren. Dette skyldes at temperaturen danner lagdeling i vannsøylen og fytoplankton har våroppblomstring. Interaksjon mellom makroalger og fytoplankton kan oppstå når de lever i samme miljø og bruker de samme ressursene for vekst og andre metabolske prosesser. En slik interaksjon har skapt bekymring for at kultivering av makroalger kan ha en negativ påvirkning på økosystemet.

Formålet med denne masteroppgaven var å undersøke om fytoplankton og *Saccharina latissima* konkurrerer om næringsstoffer, og for å se om gjødsling kan øke næringsstatusen, vekstraten og konkuransedyktigheten til *S. latissima*. For å undersøke dette ble det utført et eksperimentelt gjødslingsforsøk i et utendørs sjøvannsbasseng i Trondheim, fra slutten av februar til begynnelsen av juli. Eksperimentet inneholdt to behandlinger av *S. latissima*; en kontroll gruppe (CTL) med uforstyrret sporofytter i bassenget, og en gruppe med sporofytter som ble gjødslet (FER) i en ekstern tank i 24 og 48 timer. FER sporofyttene ble gjødslet med uorganisk nitrat (NO_3^-) og fosfat (PO_4^{3-}). Intracellulært næringsinnhold, netto opptak og vekstrate i de to behandlingene ble undersøkt og sammenliknet med næringstatusen og veksten til fytoplankton.

Resultatene viste at fytoplankton hadde maksimal vekst og høy biomasse igjennom hele eksperimentet og var derfor upåvirket av *S. latissima*. Ved hjelp av Droop-modellen ble en korrelasjon mellom spesifikk veksthastighet og intracellulære næringsinnhold i *S. latissima* etablert, der de unge sporofyttene målt i vinterperioden hadde høyest intracellulære næringsinnhold (Q_m) som førte til maksimal veksthastighet (μ_{max}). De høye næringsverdiene indikerte at sporofyttene hadde høyest lagringskapasitet i vinterperioden og at den intracellulære næringen ble brukt til vekst når næringskonsentrasjonen i vannet sank. Resultatene viste også en signifikant forskjell mellom vekst, helse og næringsinnhold i CTL og FER sporofyttene i juni. CTL sporofyttene som ikke ble gjødslet og levde i samme miljø som fytoplankton hadde sterk næringsmangel, nedgang i vekst, opptak av næring, klorofyll *a* og vev med lav eller ingen fotosyntetisk aktivitet. FER sporofyttene, hadde derimot et positivt netto næringsopptak, vekst, fotosyntetisk aktivitet og viste økte intracellulære næringsstoffverdier. Disse resultatene antyder at det er en konkurranse mellom *S. latissima* og fytoplankton når det kommer til opptak av næringsstoffer fra omgivelsene. I tillegg økte konkurransedyktigheten til opptak av næring i *S. latissima* ved at de ble eksponert for høye næringsstoffkonsentrasjoner.

Table of Contents

List of Figures	ix
List of Tables.....	xiii
1 Introduction	1
1.1 Seaweed cultivation.....	1
1.2 Seaweed cultivation in Norway.....	2
1.2.1 <i>Saccharina latissima</i>	2
1.3 Growth dependent factors for seaweed	4
1.4 Aim of the project	6
2 Material and Methods	7
2.1 Experimental discription	7
2.1.1 Preparation of the seeded lines of <i>Saccharina latissima</i>	7
2.1.2 Experimental set up	7
2.2 Description of the work and sampling methods	8
2.2.1 Seawater sampling	10
2.2.2 Sampling of sporophytes.....	10
2.2.3 Growth measruments	11
2.3 Analytical methods	12
2.3.1 Inorganic nitrate and phosphate	12
2.3.2 Total carbon and nitrogen	13
2.3.3 Total phosphorus	13
2.3.4 Chlorophyll <i>a</i>	14
2.3.5 PAM-fluorescence.....	15
2.3.6 Length measurements	15
2.3.7 Net uptake rate.....	15
2.3.1 Relationship between intracellular nutrient contents and the specific growth rate	16
2.4 Statistics.....	16
3 Results	17
3.1 Environmental conditions	17
3.2 Water samples.....	17
3.3 Nutrient uptake in <i>Saccharina latissima</i> during fertilization	21
3.4 Elemental composition of the sporophytes.....	22
3.5 Sporophyte growth	27
3.6 Net uptake of nurtrients	28
3.7 Relationship between intracellular nutrient contents and specific growth rate...30	

3.8	Sporophyte health.....	32
4	Discussion.....	33
4.1	Physical conditions	33
4.2	Environmental state of phytoplankton	34
4.3	Nutrient uptake and nutrient storage of <i>S. latissima</i>	35
4.3.1	The fertilization treatment of FER sporophytes	36
4.4	Sporophyte growth and health	36
4.5	Relationship between intracellular nutrient contents and specific growth rate...37	
5	Conclusion	38
	References	39

List of Figures

Figure 1.1: The life cycle of *S. latissima*. Figure taken from: Skjermo et al. (2014) p.13. 3

Figure 1.2: A Sporophyte thallus of *S. latissima*. The different parts of the thallus (Lamina, Holdfast and Stipe) are marked. Picture and illustration by Nora Rønningen, 2023. 4

Figure 2.1: The experimental setup was divided into the three sections, A, B and C. A: Part of the basin used for length measurements, there are two lines in section A, one line to measure the length of the control sporophytes (A:CTL) and one for the sporophytes that was fertilized (A:FER). B: shows the part of the basin used for measuring the chemical compositions of the sporophytes. There are two lines in section B too, one to measure the chemical composition of the control (B:CTL) and the fertilized sporophytes (B:FER). C: shows the external tank used to fertilize the A:FER and B:FER after the demise of the spring bloom. The picture in section C includes the water pump used to pump water into the tank from the basin. The floaters (red dots) and the weight elements (grey triangle) were placed out to structure the set up. 8

Figure 2.2: Timeline of the experiment showing the different four stages, acclimatization, before the spring bloom, the fertilization and after fertilization experiment. There were in total 13 sampling dates, where 8 of them consisted of fertilization treatments. 9

Figure 2.3: The picture to the left shows the bucket with aluminum foil that was used to collect the kelp samples from the two treatments. The picture on the right shows the aluminum foil with one of the six samples and the Mettler Toledo ME Analytical balance. Pictures taken by Nora Rønningen, 2022. 11

Figure 2.4: An example of how the individual sporophytes were marked and the pictures used to measure the length in two different days. The numbers show the individual sporophytes that were measured every sampling day. Pictures taken by Nora Rønningen, 2022. 12

Figure 3.1: Environmental conditions in the seawater basin from the end of february to the beginning of July. A: The temperature ($^{\circ}\text{C}$) in the basin and B: the salinity (ppt) in the basin. The gray dotted line symbolizes the demise of the spring bloom. 17

Figure 3.2: Nutrient and chlorophyll *a* concentration in the seawater basin in the period late February 2022 to early July 2022. A: Nitrate ($\mu\text{g NO}_3\text{-N L}^{-1}$), B: Phosphate ($\mu\text{g PO}_4\text{-P L}^{-1}$), C: chlorophyll *a* ($\mu\text{g L}^{-1}$), D: Particulate organic carbon ($\mu\text{g POC-C L}^{-1}$), E: Particulate organic nitrogen ($\mu\text{g PON-N L}^{-1}$) and F: Particulate organic phosphorus ($\mu\text{g POP-P L}^{-1}$), with standard error of the mean ($n=3$). The gray dotted line symbolizes the demise of the spring bloom. 18

Figure 3.3: Elemental ratios of phytoplankton $<200\ \mu\text{m}$ in the seawater basin in the period late February 2022 to early July 2022. A: Nitrogen: Carbon ratio ($\mu\text{g N mg}^{-1}\text{ C}$), B: Phosphorous: Carbon ratio ($\mu\text{g P mg}^{-1}\text{ C}$) and C: Nitrogen: Phosphorous ratio ($\mu\text{g N }\mu\text{g}^{-1}\text{ P}$) with standard error of the mean ($n=3$). The gray dotted line symbolizes the spring bloom. 20

Figure 3.4: Inorganic nutrient contents in the tissue of *S. latissima* from the different treatments in the period from the end of February to the beginning of July. A: Nitrate (μg

NO₃-N mg⁻¹ DW) and B: Phosphate (µg PO₄-P mg⁻¹ DW). Left panels: from late February until demise of spring bloom. Right panel: from demise of spring bloom till early July. The gray dotted line separates the graphs before and after the spring bloom and the scale of the y-axis. The arrow marks when the fertilization doze and incubation time increased. Error bars express standard error of the mean (n=3).23

Figure 3.5: Total tissue contents of nutrients and chlorophyll *a* in the different treatments of *S. latissima* in the period from late February to beginning of July. A: Total intracellular nitrogen (Q_N, µg N mg⁻¹ DW), B: Total intracellular phosphorus (Q_P, µg P mg⁻¹ DW), C: Total intracellular carbon (Q_C, µg C mg⁻¹ DW) and D: Chlorophyll *a* (µg Chl *a* mg⁻¹ DW). Left panels: from late February until demise of spring bloom. Right panel: from demise of spring bloom till early July. The gray dotted line separates the graphs before and after the spring bloom and the scale of the y-axis. The arrow marks where the fertilization doze and incubation time increased. Error bars express standard error of the mean (n=3).24

Figure 3.6: The elemental ratios in the tissue of *S. latissima*. A: N:C (µg N µg⁻¹ C), B: P:C (µg P µg⁻¹ C) and C: N:P (µg N µg⁻¹ P). Left panels: from late February until demise of spring bloom. Right panel: from demise of spring bloom till early July. The gray dotted line separates the graphs before and after the spring bloom and the scale of the y-axis. The arrow marks where the fertilization doze and incubation time. Error bars express standard error of the mean (n=3). The data are based on the values for Q_N, Q_P and Q_C shown in figure 3.5 A-C and Table 3.5.26

Figure 3.7: The length (cm) of the sporophytes before the spring bloom, and for FER and CTL treatment in the period from late February to early July. Left panels: from late February until demise of spring bloom. Right panel: from demise of spring bloom till early July. The gray dotted line separates the graphs before and after the spring bloom. Error bars express standard error of the mean (n=81 for CTL and 103 for FER) with data smoothing. The arrow marks when the fertilization doze and incubation time increased (Table 2.1).27

Figure 3.8: The absolute and specific growth rates of the sporophytes from the end of February 2022 to the beginning of July 2022. A: Absolute growth rate (cm day⁻¹) and B: Specific growth rate (µ, day⁻¹). Left panels: from late February until demise of spring bloom. Right panel: from demise of spring bloom till early July. The gray dotted line separates the graphs before and after the spring bloom and the arrow marks when the fertilization doze and incubation time increased.28

Figure 3.9: The net uptake of nutrients during the experiment. A: net uptake of nitrogen (V_N, µg N mg⁻¹ DW day⁻¹) and B: net uptake of phosphorus (V_P, µg P mg⁻¹ DW day⁻¹). Left panels: from late February until demise of spring bloom. Right panel: from demise of spring bloom till early July. The gray dotted line separates the graphs before and after the spring bloom and the scale of the y-axis. The arrow marks when the fertilization doze and incubation time increased. Error bars express standard error of the mean (n=3).29

Figure 3.10: The Droop-model. A-B: The specific growth rate of *S. latissima* sporophytes (µ, day⁻¹) as a function of the intracellular nutrients contents (Q_x), with the Q_m and µ_{max} marked in red and the hyperbola Droop-graph in green. A: intracellular nitrogen contents (Q_N, µg N mg⁻¹ DW) ad B: Intracellular phosphorous content (Q_P, µg P mg⁻¹ DW). The error bars are the standard error of mean (SE, n=3). C-D: The transformation done to find the Droop-equation, which was the intracellular nutrient content of *S. latissima* (Q_x) times the specific growth rate (µ, day⁻¹) as a function of the intracellular nutrient contents (Q_x), with linear regression and the 95% confidence interval marked in green dotted line. C: is for the intracellular N contents (Q_N, µg N mg⁻¹ DW) and B: is for the intracellular P content

(Q_p , $\mu\text{g P mg}^{-1}\text{ DW}$). The data points are all the positive values measured of *S. latissima* from the different treatment combined.....31

Figure 3.11: The PAM-fluorescence (F_v/F_m) in sporophytes from FER and the CTL sporophytes in June 2022. The orange bars and the upper picture (ABC) are the FER and the blue bars, and the bottom picture (abc) are the CTL. The sporophytes were divided into three sections where the measurement were done upper part of the lamina (A,a), middle part of the lamina (B,b) and the tip of the lamina (C,c) part of the lamina as shown in the pictures. Error bars express standard error of the mean ($n=9$).....32

List of Tables

Tabell 2.1: The total concentration and doze of nitrate and phosphate added in the eight different fertilizations. The sporophytes were fertilized with NaNO_3 and KH_2PO_4 , and the doze increased with time during the spring. The incubation time also increased throughout the spring. During every fertilization the tank with sporophytes were fertilized in the morning and in the evening, and the total concentration added is the sum. 9

Tabell 3.1: The mean values and the standard error of the mean of the total particulate organic compounds, extracellular concentrations of inorganic nutrients and chlorophyll *a* concentration of phytoplankton in the seawater basin in the period late February 2022 to early July 2022. The data is divided into before and after the spring bloom. The data is based on the graphs in Figure 3.2. (n=5-16 Before spring bloom, n=20-27 after spring bloom)19

Tabell 3.2: The mean elemental ratios of PON:POC, POP:POC and PON:POP in the seawater basin before and after the spring bloom with standard error of the mean (n=10 Before spring bloom and n=18 After spring bloom). The data is based on the graphs in Figure 3.3.20

Tabell 3.3: The inorganic nitrate concentration and uptake in the fertilization tank during the eight fertilizations, with the total inorganic nitrate concentration ($\mu\text{g L}^{-1}$) added to the tank, the concentration in the tank water ($\mu\text{g L}^{-1}$) before the fertilization were added (basin water), the nutrients taken up from the tank during fertilization per day ($\mu\text{g L}^{-1} \text{ day}^{-1}$). Nitrate was added in Redfield proportions.21

Tabell 3.4: The inorganic phosphate concentration and uptake in the fertilization tank during the eight fertilizations, with the total inorganic phosphate concentration ($\mu\text{g L}^{-1}$) added to the tank, the concentration in the tank water ($\mu\text{g L}^{-1}$) before the fertilization were added (basin water), the nutrients taken up from the tank during fertilization per day ($\mu\text{g L}^{-1} \text{ day}^{-1}$). Phosphate was added in Redfield proportions.22

Tabell 3.5: The mean values and the standard error of the mean for the total tissue contents of nutrients (Q_N , Q_P and Q_C), inorganic nutrients ($\text{NO}_3\text{-N}$ and $\text{PO}_4\text{-P}$) and chlorophyll *a* in the different treatments of *S. latissima* in the period from late February to beginning of July. (n=14-27). The data is based on the graphs in Figure 3.4 and 3.5.25

Tabell 3.6: The mean values and the standard error of the mean for the elemental ratios of N:C ($\mu\text{g N mg}^{-1} \text{ C}$), P:C ($\mu\text{g P mg}^{-1} \text{ C}$) and N:P ($\mu\text{g N } \mu\text{g}^{-1} \text{ P}$) in the different treatments of *S. latissima* in the period from late February to beginning of July. The data is based on the graphs in Figure 3.6. (n=12 before the spring bloom and n=24 for CTL, FER and Fertilized-FER)26

Tabell 3.7: The mean values and the standard error of the mean for the net uptake of nitrogen ($\mu\text{g N mg}^{-1} \text{ DW day}^{-1}$) and phosphorus ($\mu\text{g P mg}^{-1} \text{ DW day}^{-1}$) and the ΔQ in the different treatments of *S. latissima* in the period from late February to beginning of July. The data is based on the graphs in Figure 3.9 and is calculated with Equation 2.11 (n=12 and 24).30

Tabell 3.8: The values of Q_0 , μ'_{\max} , Q_m and μ_{\max} for both the Q_N and Q_P , based the Droop-model in Figure 3.10. The values were calculated form Equation 1.1 and 2.13. (mean \pm SE, $n=3$ and $n=2$ (Q_0 , μ'_{\max}) and $n=8$ (Q_m , μ_{\max})).....31

1 Introduction

1.1 Seaweed cultivation

Human population is growing, and the concern of providing sufficient amount of food and resources are increasing correspondingly (Miller, 2008). The United Nations (UN) estimated that the human population will reach 9.7 billion by 2050 (UN, 2019). To be able to feed the growing population it is needed to increase the global food production 70% by 2050 (Ghose, 2014, Skjermo et al., 2014). For centuries agriculture and fisheries have supplied people with food and resources, however, with a growing human population, the demand for living area increases, giving less space for agricultural activity. In addition, with climate change and human overpopulation the supply of freshwater for drinking and agriculture gets limiting (Ytrestøyl et al., 2015). Fisheries have also been a vital source for food for humans. However, due to few fishing licenses and fishing quota in the past the fish stocks in the ocean have been overexploited (Olsen, 2011). In 2006 the Food and agriculture organization (FAO) proposed cultivation of the sea and aquaculture as an industry that have the potential to make a large contribution in producing food in the future (FAO, 2006).

Seaweed cultivation has a low environmental impact in the marine ecosystem (Slegers et al., 2021), with no use of fertilizers or chemicals to grow (Hancke et al., 2018). They are phototrophic organisms that produce chemical energy and oxygen by absorbing sunlight, nutrients and carbon dioxide from the water through photosynthesis (Hancke et al., 2018, O'Connor, 2017). Thus, they also play an important role in mitigating negative effects caused by climate change as a part of the carbon sequestration, contributing to a local mitigation of ocean acidification (Duarte et al., 2017). Recent studies have also shown that by using seaweed as a component in feed to ruminants such as cows, the enteric methane production gets lower (Abbott et al., 2020, Lean et al., 2021). Methane is a natural gas that is a largely potent greenhouse gas that traps heat in the atmosphere at higher rate than carbon dioxide (Howarth, 2014). In addition to being important for the environment, seaweed is a potential source for food and other products important for human consumption and can therefore be an important source for the food security of the growing human population (Skjermo et al., 2014).

Humans have utilized seaweed as a source of food, medicine, fertilizer and animal feed for over 1300 years in coastal communities (Dillehay et al., 2008). Seaweed has biochemical composition and structure, such as polysaccharide, protein, vitamins, minerals and n3 fatty acids that can be exploited (Kumar et al., 2008). Seaweed has a unique polysaccharide structure called hydrocolloids that can be extracted from the tissue with today's technology. The most used hydrocolloids are alginate, carrageenan, and agar (Bartsch et al., 2008, Hentati et al., 2020). These structures are water-binding and have thickening properties that can be used in different foods such as stews and sauces, cosmetics, in bacteria culture medium used in medical and biological research and bioplastic film used to make packaging among other things (Dhargalkar and Pereira, 2005, Kumar et al., 2008, Buchholz et al., 2012, Lim et al., 2018). Seaweed can also be used in making biofuel (Kraan, 2013) and has also cellulose-like fibers that can be used to make textile (Buchholz et al., 2012). There is a large potential for producing sustainable products by using

seaweed as a component, that can contribute to reach the UN Global Sustainable Development Goals.

There are registered around 10,000 different species of macroalgae divided into three groups based on the color of the main pigmentations, including: red, brown, and green algae (O'Connor, 2017). The red algae are the most diverse group, and some genus such as *Kappaphycus*, *Gracilaria* and *Euclima* are cultivated in a large scale in Asian countries (O'Connor, 2017, Cai et al., 2021). Brown algae on the other hand includes the kelp family (O'Connor, 2017). Kelp (*Laminariales*) is naturally found in cold waters and is the order of seaweed that has the highest production in Norway (Skjermo et al., 2014). The green algae are the seaweed found in the upper littoral zone and are cultivated in a small scale (O'Connor, 2017, Cai et al., 2021). Out of the around 10,000 species, 221 of them have commercial value globally (FAO, 2018).

FAO (2020) stated that out of the total global seaweed harvest, both harvest from natural wild-living populations and farmed, 97.1 percent of the harvest was farmed seaweed. The last couple of decades the production of seaweed has increased from 10.6 million tons in 2000 to 32.4 million tons in 2018 (FAO, 2020). The majority of the production takes place in East and southeast Asia and contribute to over 97 percent of the large-scale seaweed farming globally in 2019, with most production of red and brown macroalgae (FAO, 2018, Cai et al., 2021). Although, the majority of the seaweed produced in the world comes from Asia, the interest and production of seaweed is rising in Europe due to the wide variety of sustainable products seaweed can be used in (Van den Burg et al., 2021). The total production of seaweed in Europe was 287,033 tons in 2019, and the production has increased since then (Cai et al., 2021). In Europe, Norway was the leading country in 2019 when it comes to cultivation of seaweed and other aquatic plants, followed by France and Ireland (Cai et al., 2021, FAO, 2021, Van den Burg et al., 2021).

1.2 Seaweed cultivation in Norway

In Norway, seaweed have been utilized industrially for several decade with harvesting natural seaweed. However, the first commercial licenses to cultivate kelp came in 2014 (Hancke et al., 2018). The number of sites and permits have increased ever since, with 54 licenses in 2014 and 539 license in 2023 (Directorate of Fisheries, 2023). Norway has a long coastline with good water quality and optimal physico-chemical parameters extending over 100,000 km with many deep fjords, islands, and sheltered bays, that creates areas suitable for seaweed cultivation (Skjermo et al., 2014, Stévant et al., 2017, Hancke et al., 2018). The most popular species to cultivate in Norway are *Saccharina latissima* (sugar kelp) and *Alaria esculenta* (winged kelp) (Skjermo et al., 2014), where 96% of the total cultivation of seaweed in Norway is production of *S. latissima* (Hancke et al., 2018). *S. latissima* is not only cultivated in Norway but is also one of the most popular cultivated species in Europe, with a total production of 1000 tons in 2018 (FAO, 2018).

1.2.1 *Saccharina latissima*

Saccharina latissima (Linnaeus, Lane, Mayes, Druehl and Saunders) is the most popular fast-growing specie to cultivate in Norway and Europe because of its many good qualities (Lane et al., 2006, Hancke et al., 2018). The species has high content of minerals, protein, lipids and fiber (Neto et al., 2018). *S. latissima* is a brown algae in the family *Laminariaceae*, and it is commonly called sugar kelp due to its sweet taste when dried into powder (White and Marshall, 2007, Skjermo et al., 2014). In nature, this specie lives in rocky sublittoral areas in temperate to polar regions, with a natural distribution from

Portugal in the south to Spitsbergen in the north (Van den Hoek and Donze, 1967, Moy and Christie, 2012). *S. latissima* prefers areas with moderate currents and movements in the water, has an optimal temperature that ranges from 10-15 °C (Bolton and Lüning, 1982), an optimal light intensity of 110 $\mu\text{mol m}^{-2} \text{s}^{-1}$ (Fortes and Lüning, 1980) and an optimal salinity between 27-33 ppt (Nielsen et al., 2016). To avoid strong wave exposure while at the same time getting enough light, *S. latissima* lives naturally in depth from 0-30 meters, depending on the habitat (Skjermo et al., 2014). *S. latissima* can reach length up till 3-4 meters and has a high growth rate from late winter to spring. The growth rate is normally about 1.1 cm day^{-1} , although, growth rate up to 4.87 cm day^{-1} have been documented (Sjøtun, 1993).

Unlike terrestrial plants, the mature *S. latissima* is called a sporophyte because it contains sorus with zoospores that turns into female or male gametophytes (Visch et al., 2019). In the nature, the formation of the spores are temperature sensitive and happens normally in the winter period when the water temperature is low (Skjermo et al., 2014). (Figure 1.1)

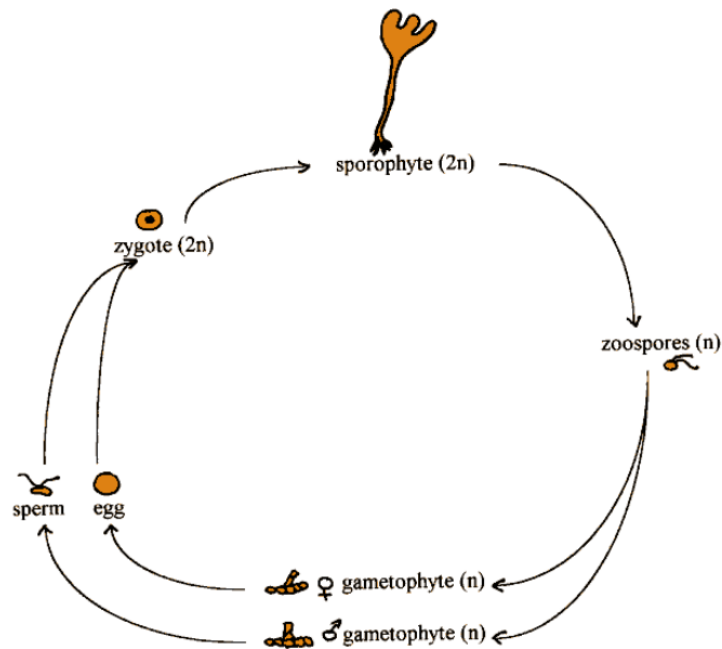


Figure 1.1: The life cycle of *S. latissima*. Figure taken from: Skjermo et al. (2014) p.13.

The sporophyte consists of different parts, which is shown in Figure 1.2. The blade-like structure of the sporophyte is called lamina and is where photosynthesis takes place. When the sporophyte grows, the new tissue is formed by the stipe, meaning that the oldest part of the lamina is in the end of the thallus (Figure 1.2). To be able to live in rocky areas, the sporophyte has an organ called holdfast, which holds the sporophytes to rocks or other solid structures (Lane et al., 2006).

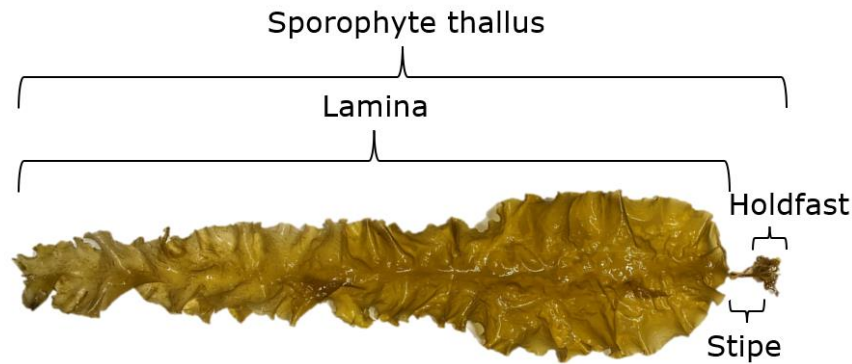


Figure 1.2: A Sporophyte thallus of *S. latissima*. The different parts of the thallus (Lamina, Holdfast and Stipe) are marked. Picture and illustration by Nora Rønningen, 2023.

1.3 Growth dependent factors for seaweed

To optimize the production of seaweed it is important to understand what environmental conditions the seaweed needs to optimize growth and health (Hurd et al., 2014). The key elements that are essential for growth are resources of nutrient and light availability (Forbord et al., 2021). Other factors such as the site's topography, salinity and temperature have also an effect on the growth (Hurd et al., 2004).

There are five major elements all organisms living on earth are made up on, C, H, O, P and N. Nitrogen (N) and phosphorous (P) are macronutrients which seaweed, and other photosynthetic organisms, needs to grow, do photosynthesis and reproduce. The nutrients in seawater can be in different forms. Nitrogen and phosphorus can firstly be in particulate organic form (PON and POP), secondly dissolved organic (DON and DOP) and finally dissolved inorganic forms (DIN and DIP). There are different forms of the dissolved inorganic nutrients, where DIN can be nitrate (NO_3^-), nitrite (NO_2^-) or ammonia (NH_4^+) depending on which state the nutrients are in the nitrification. The DIP conducts of different orthophosphate where some is bound to hydrogen, but the simplest form is phosphate (PO_4^{3-}) (Sarmiento and Gruber, 2006).

The nutrient concentrations in the ocean are controlled by physical and biological processes. In temperate areas such as Norway there is a seasonality in the light and nutrient availability. In the winter, sunlight is limited and in the summer the availability of light is high. It is the opposite for nutrients, where the availability is high in the winter and low in the summer. The seasonality in nutrients is due to physical mixing or stratification during the seasons. During the summer there is a stratification in the water column, where the surface water is warmer than the deep water. However, when the surface water gets colder in the autumn and winter the stratification decreases, leading to a vertical mixing of the water columns (Rey, 2004).

Although the nutrient concentration is high in the winter, the light availability is low. *S. latissima* as well as the rest of the macroalgae, need the combination of light and nutrients to be able to grow via photosynthesis. When the sunlight and temperature increase in the spring, the water column gets stratified, so nutrients are available for photosynthetic organisms. However, due to the combination of nutrients and light, phytoplankton take advantage of the situation, and grow faster than the seaweed. This causes a nutrient limitation for seaweed, while phytoplankton grows (Rey, 2004, Forbord et al., 2021). This event is called phytoplankton bloom (Rey, 2004). In this context, since seaweed and

phytoplankton are living naturally in the same environment and uses the same resources for growth; there has been a concern that macroalgae farming can negatively affect the growth of the phytoplankton bloom competing for nutrients (Aldridge et al., 2021, Semerciöz et al., 2021).

When inorganic nutrients are taken up by the seaweed, the nutrient are transformed into an organic form (Naldi and Viaroli, 2002). *S. latissima* store nitrogen in intracellular pools located in the vacuoles in the plant cell (Hurd et al., 2014). The seaweed incorporates the nitrogen in the vacuole when the uptake of nitrate is greater than the conversion rate to nitrite (Harrison and Hurd, 2001). The intracellular nitrogen can reach higher levels than in the surrounding water, with the highest storage in the winter, when the nitrate in the water is high, due to active transport (Chapman and Craigie, 1977, Hurd et al., 2014). With increased internal pools of NO_3^- , the photosynthesis in *S. latissima* increases correspondingly (Chapman et al., 1978). Phosphorus storage in *S. latissima* is less investigated, but different species have different storage capacity (Pedersen et al., 2010).

The internal content of nutrients is depended on both the ambient concentration of nutrients, the uptake rate and storage. Jacques Monod developed a model to describe growth of microorganisms based on the external concentration of limiting nutrients (Liu, 2007). However, the Monod-model did not take the internal content of nutrient into account, and pronounced variability of external concentrations over short time, which reduced later application of the model. The Droop-model, on the other hand, describe growth rate as a function of the internal content of the limiting nutrient (Droop, 1974). The droop-model are shown in Equation 1.1 and Table 1.1 explains the different symbols.

$$1.1 \quad \mu = \mu'_{max} \left(1 - \frac{Q_0}{Q}\right)$$

A graph for the range of Q-values versus their specific growth rate will according to Equation 1.1 form a hyperbola growth curve, which makes it possible to estimate Q_m which is the internal content that gives maximum growth (μ_{max}) (Droop, 1974). The Droop-model were established for microorganisms, but efforts are made to show that it can be used for seaweed as well (Kopczak et al., 1991, Hafting, 1999, Njåstad et al., in progress).

Table 1.1: Symbols used in the Droop-model (Equation 1.1)

Symbols used in the Droop-model	
μ	Specific growth rate (μ , day ⁻¹) (Equation 2.10)
Q	The internal nutrient content of nitrogen (Q_N) or phosphorus (Q_P).
Q_0	The minimum internal nutrient content that allows net positive growth.
μ'_{max}	The maximum apparent specific growth rate for infinite internal nutrient content
Q_m	The internal content that gives maximum growth (μ_{max}) (Figure 3.10).
μ_{max}	The maximum specific growth (Figure 3.10).

1.4 Aim of the project

Seaweed and phytoplankton lives in the same environment and compete over the same inorganic nutrient resources for growth and reproduction. The main aim of this study was to investigate if there is a competition for inorganic nutrients between *Saccharina latissima* and phytoplankton, and how a fertilization treatment with additional nutrients may increase the nutritional state and growth rate, and then the competitive ability of *S. latissima*.

Based on earlier studies, we expected that *S. latissima* may experience severe nutrient limitation, after the spring bloom, and aimed to provide further evidence for this. We also hypothesized that sporophytes of *S. latissima* treated regularly with seawater enriched with nutrients after the spring bloom will show a higher intracellular nutrient content and growth rate than the sporophytes of *S. latissima* kept as unfertilized control, competing with the phytoplankton.

To provide answers to the aim of the project, two sub-objectives were established:

- 1) To determine and evaluate the competitive ability for nutrients of *S. latissima* with the phytoplankton community during the spring.
- 2) To assess and evaluate the growth and nutritional state of *S. latissima* under two different treatments, one fertilized group with additional boost of nutrients and one control group without any treatment.

2 Material and Methods

2.1 Experimental discription

2.1.1 Preparation of the seeded lines of *Saccharina latissima*

Sporophytes of *Saccharina latissima* with sorus were collected from a wild growing population close to Frøya in Norway. The sori was induced to release the zoospores at Seaweed Solutions laboratory in Trondheim. The zoospores were fertilized, and the young new sporophytes were attached to polyester line (6mm), which was coiled around a Plexiglas coil. After incubation in approximately 8 weeks in a 300 L tank with continuous water flow at 10-12 °C with 10-20 $\mu\text{mol m}^{-2} \text{s}^{-1}$ light intensity the sporophytes had reached a length of 0-4 cm. The Seeded lines with *S. latissima* were transported from the Seaweed Solutions hatchery in January 2022 to Trondheim Biological Station (TBS) in a Styrofoam box.

The seeded lines were cut in 32 segments of 1m with around 90-100 sporophytes divided into 5 marked clusters and kept in a tank with seawater exchanged by water taken from 80m depths. The sporophytes were kept overnight until they were connected to ropes in the basin (Figure 2.1). The 32 segments of seeded lines were selected and connected to four different ropes treated differently (see section 2.1.2 for more details). The ropes were climatized in the basin for approximately three weeks (22 days) before the first sampling were undertaken.

The ropes were attached to the banister in the basin and lowered to 1-2 m deep to avoid irradiation from the sun. Floaters and weight elements were attached to the rope to keep the rope at a stable deep.

2.1.2 Experimental set up

The experiment was set up in an outdoor seawater basin at Trondheim Biological Station (TBS) located at Trolla in Trondheim (Norway). The seawater used in the basin was pumped in from the Trondheim fjord from 80m deep, with little water flow simulating and leading to the stratification that happens naturally in the fjord during the spring. The experiment was conducted from January to July 2022.

The experiment involved different treatments;

- 1) Sporophytes maintained in undisturbed conditions inside the basin as a control (CTL).
- 2) Sporophytes maintained in the basin and fertilized with inorganic nutrients (FER) for 24 and 48 h in an external tank from after the spring bloom (6th of April) till the end of the experiment. The nutrient concentration in the tank was increased with time.
- 3) The two treatment groups were sampled, and length measured at the same time, right before fertilization treatment, but the FER sporophytes were also sampled immediately after fertilization, constituting a third treatment group (Fertilized-FER).

The sampled sporophytes were analyzed for determination of chemical C, N and P composition of sporophytes of the treatment groups. Parallel to the sampling, length measurements were made for the CTL and FER. The sporophyte used for sampling were

separated from the sporophyte used for length, see details below. The experimental set up is shown in Figure 2.1 where the basin is divided into two sections, one for length measurements (A) and one for chemical analysis (B), with one rope from each treatment in each section. The external fertilization tank (480L) (C) was placed on the side of the basin. The water used in the tank was pumped in from the basin at around 1.5m dept. During every fertilization treatment the tank was enriched with phosphate and nitrate. The fertilization doze was prepared in a 1L glass bottle with 0.85 g NaNO_3 and 0.085 g KH_2PO_4 dissolved in 1L of MQ water. The nutrient concentration in the bottle was 10mM NO_3^- and 0.625mM PO_4^{3-} , and by giving 0.5 L of the bottle the concentration in the tank became $10\mu\text{M NO}_3^-$ which is the concentration in deepwater and that was used by Forbord et al. (2021). The relationship between NO_3^- and PO_4^{3-} was 1:16 (Redfield, 1963).

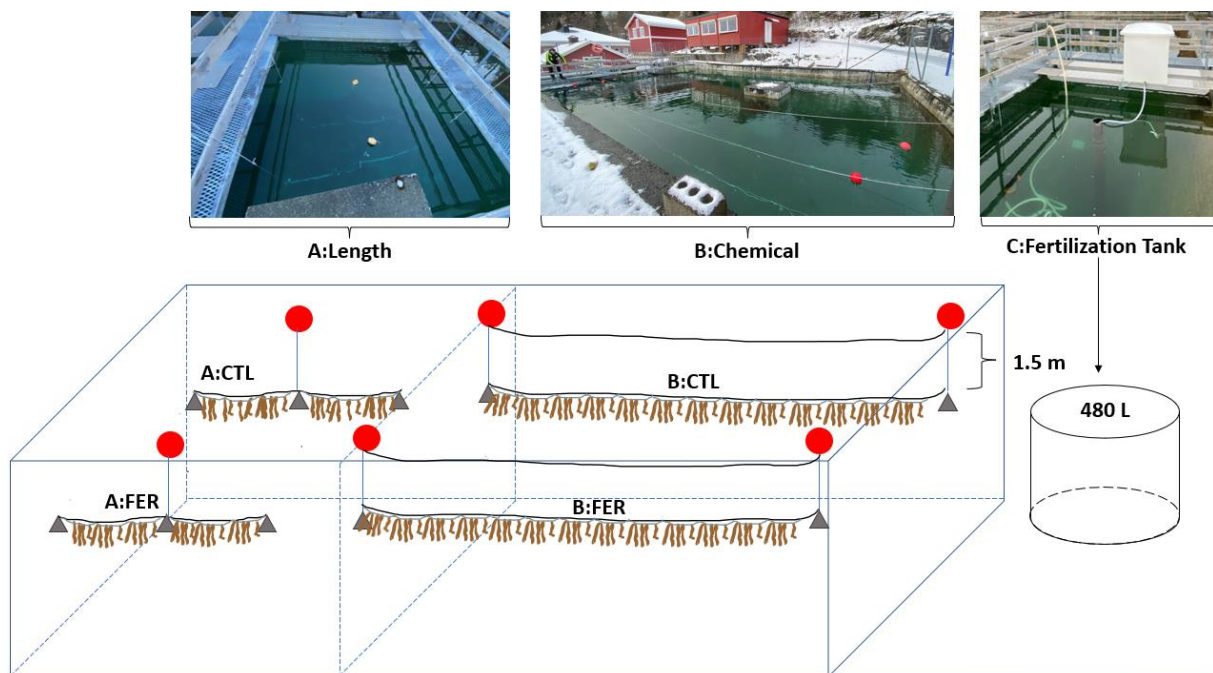


Figure 2.1: The experimental setup was divided into the three sections, A, B and C. A: Part of the basin used for length measurements, there are two lines in section A, one line to measure the length of the control sporophytes (A:CTL) and one for the sporophytes that was fertilized (A:FER). B: shows the part of the basin used for measuring the chemical compositions of the sporophytes. There are two lines in section B too, one to measure the chemical composition of the control (B:CTL) and the fertilized sporophytes (B:FER). C: shows the external tank used to fertilize the A:FER and B:FER after the demise of the spring bloom. The picture in section C includes the water pump used to pump water into the tank from the basin. The floaters (red dots) and the weight elements (grey triangle) were placed out to structure the set up.

2.2 Description of the work and sampling methods

The experiment lasted for 6 months with 13 sampling days. At every sampling day, sporophytes were sampled for chemical content of N, P and C and chlorophyll *a* (Chl *a*), length measurements were made and water samples from basin were taken to measure the N, P and C content in phytoplankton and the dissolved inorganic nutrient concentration in the water. In addition, samples of the tank water were taken to estimate the uptake of nutrients during fertilization. Salinity and temperature of the seawater in the basin were also taken every sampling.

Figure 2.2 shows the timeline of the experiment. The experiment was divided into four stages: 1) acclimatization, 2) before the demise of the spring bloom 3) sporophytes from FER were treated with nutrient enriched seawater or fertilized 4) a period after fertilization incubations. During the “before spring bloom” stage four samplings were done, during the fertilization trail eight samplings were done and one sample were taken after the fertilization treatment.

The fertilization doze and incubation time was increased throughout the experiment, and are divided into three phases; simple, doble and quadrupled doze added during fertilization, where the total concentration added is explained in Table 2.1.

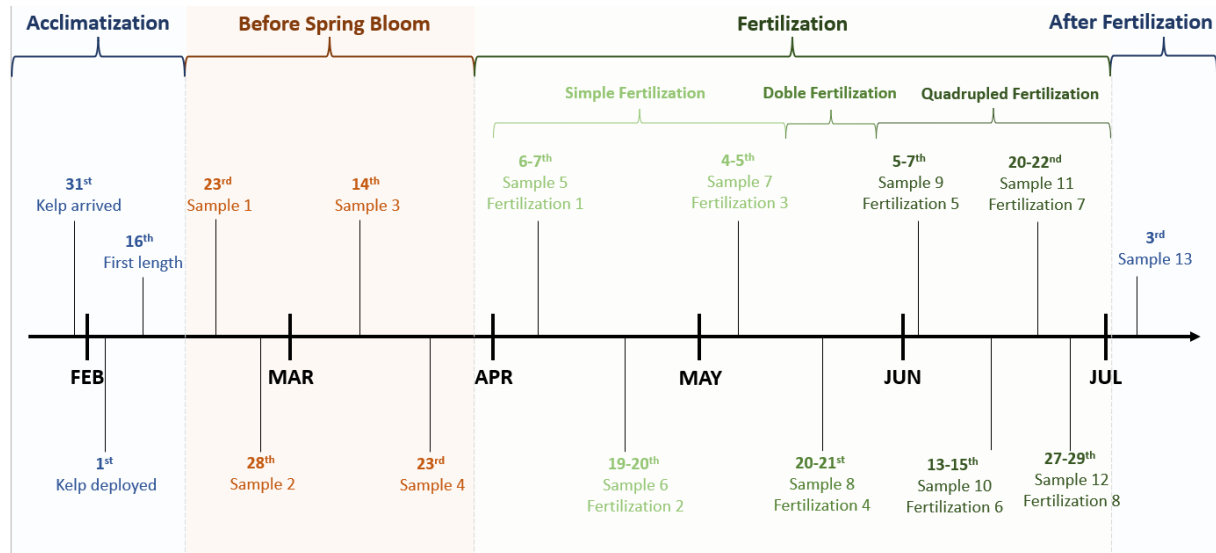


Figure 2.2: Timeline of the experiment showing the different four stages, acclimatization, before the spring bloom, the fertilization and after fertilization experiment. There were in total 13 sampling dates, where 8 of them consisted of fertilization treatments.

Tabell 2.1: The total concentration and doze of nitrate and phosphate added in the eight different fertilizations. The sporophytes were fertilized with NaNO_3 and KH_2PO_4 , and the doze increased with time during the spring. The incubation time also increased throughout the spring. During every fertilization the tank with sporophytes were fertilized in the morning and in the evening, and the total concentration added is the sum.

Fertilization	Date	Incubation (h)	Total concentration added ($\mu\text{g L}^{-1}$)	
			NO_3^-	PO_4^{3-}
1	6-7 th of April	24	280	38.7
2	19-20 th of April	24	280	38.7
3	4-5 th of May	24	280	38.7
4	20-21 st of May	24	560	77.4
5	5-7 th of June	48	1120	155
6	13-15 th of June	48	1120	155
7	20-22 nd of June	48	1120	155
8	27-29 th of June	48	1120	155

2.2.1 Seawater sampling

Seawater was collected for analysis of dissolved inorganic nutrients (NO_3^- and PO_4^{3-}), total particulate carbon, nitrogen and phosphorous (PON, POC and POP), and Chl *a*. The seawater from the basin was collected using a water-tube sampler at approximately 1.5 m depth (5L). To remove the biggest particles, such as large organisms and other organic material, the seawater was filtered through a 200 μm plankton net before being transferred to a brown 10 L polycarbonate bottle.

The 200 μm filtered water was immediately filtered for analysis of dissolved and particulate variables in the laboratory by using a water filtration apparatus with glass fiber filters (GF-filters, Whatman 25 mm) that had pore size around 0,2 μm . After filtration, the filters were placed in petri dishes wrapped in aluminum foil and stored in the freezer. The samples collected on GF-filters were used to analyze the PON, POP, POC and Chl *a*. The filtered water was put in 15 ml plastic tubes were used to analyze the inorganic nutrients. Both filters and plastic tubes were stored at -20 °C in the freezer until further analysis. The salinity and temperature in the basin were measured at 1.5 meter deep by using a CTD instrument (LF 330).

2.2.2 Sampling of sporophytes

Sporophyte samples were taken for analysis of inorganic nutrients ($\text{NO}_3\text{-N}$ and $\text{PO}_4\text{-P}$), the particulate organic material (PON, POP and POC), Chl *a* and for measurement of PAM-fluorescence in the tissue. To measure $\text{NO}_3\text{-N}$ and $\text{PO}_4\text{-P}$ and PON, POP and POC in the sporophyte, a random number of individual sporophytes from FER and CTL and Fertilized-FER were collected and placed in a bucket with aluminum foil, shown in Figure 2.3. Once in the laboratory, sporophytes samples of each treatment were divided into three replicates. The three replicates from each treatment were weighted using a scale (Mettler Toledo ME Analytical balance) and dried at 60 degrees for a minimum of 24 h in a drying cabinet (Termaks). When the samples were completely dried, the replicates were weighted again to estimate of the dry weight (DW). After that, the replicates were stored in a freezer (-20°C) until further preparation. Right before the analyzation the dried samples were taken out of the freezer and grounded into a homogenized powder by using a mortar. The powder was placed in plastic tubes and stored in room temperature before analysis.

To measure the Chl *a* in the tissue, approximately 1x1cm (ca. 0.05 g) samples of fresh lamina tissue from FER and CTL sporophytes were taken. In addition, three individual sporophytes from each treatment were collected to determine the photosynthetic efficiency in the kelp using PAM-fluorescence in June. The sporophytes were put in a Styrofoam box with seawater from the basin while being transported to the laboratory. Both analysis of Chl *a* and PAM-fluorescence were done right after the sporophyte samples were taken from the basin. Se section 2.3 for more detail.

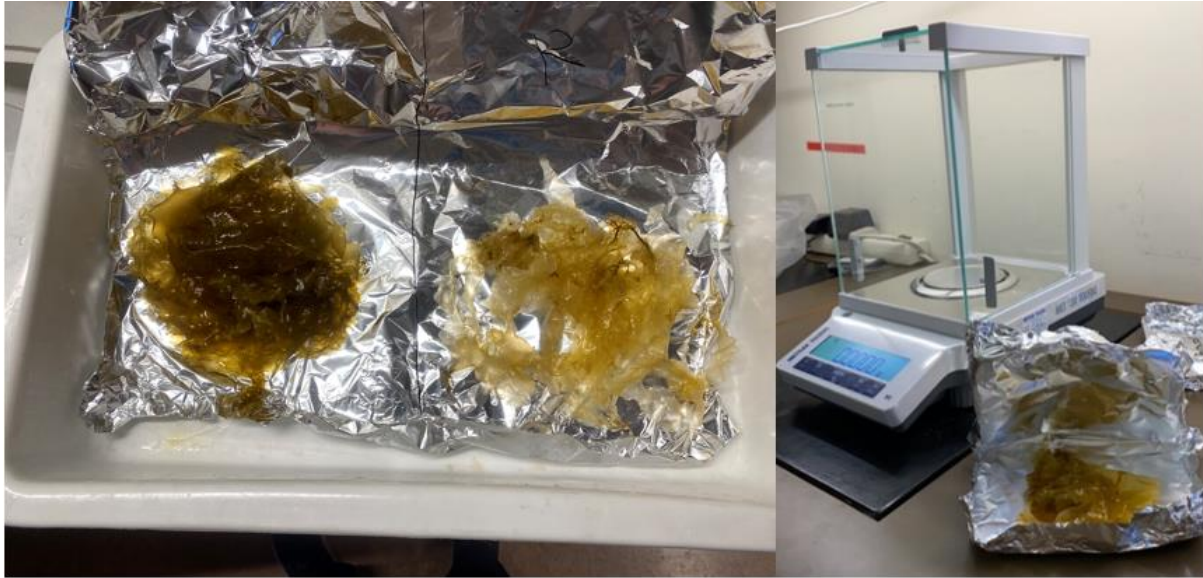


Figure 2.3: The picture to the left shows the bucket with aluminum foil that was used to collect the kelp samples from the two treatments. The picture on the right shows the aluminum foil with one of the six samples and the Mettler Toledo ME Analytical balance. Pictures taken by Nora Rønningen, 2022.

In addition, seawater samples from the external tank were also taken to measure the inorganic nutrients ($\text{NO}_3\text{-N}$ and $\text{PO}_4\text{-P}$) taken up by the sporophytes during fertilization. Samples were taken before and after every doze added to the tank. Approximately 30ml tank-water was collected in a glass beaker and filtered into 15ml plastic tubes by using a $0.45 \mu\text{m}$ syringe. The filtration was done to remove particles and larger organic components in the tank-water. The plastic tubes with filtered tank-water were store in the freezer (-20°C) for further analysis.

The analytical methods for the water samples, the GF-filters, Chl *a* and PAM fluorescence are described in detail in section 2.3.

2.2.3 Growth measurments

The length of the sporophytes was measured by taking pictures of the clusters of sporophytes from FER and CTL on a white laminated paper with a reference 1cm line (Figure 2.4). The length of approximately 30 individual sporophytes from each treatment were analyzed in Image J. The same individual sporophytes were measured every sampling day.



Figure 2.4: An example of how the individual sporophytes were marked and the pictures used to measure the length in two different days. The numbers show the individual sporophytes that were measured every sampling day. Pictures taken by Nora Rønningen, 2022.

2.3 Analytical methods

The analytical methods for analyzing nitrate, phosphate, nitrogen, phosphorous, carbon and Chl *a* in the seawater and the sporophyte tissue is similar. In this section the methodology for the analytical methods for water samples and *S. latissima* tissue will be explained together.

2.3.1 Inorganic nitrate and phosphate

The GF-filtered water and the tank-water filtered through a syringe was used to analyze the inorganic nitrate and phosphate. Thawed samples of 4 ml were analyzed in an auto analyzer (Flow Solution IV System O.I Analytical Auto analyzer) according to Norwegian standard 4745. Some of the samples taken from the fertilization tank were diluted before analysis due to high nutrient concentrations. The samples were then diluted with distilled water according to the fertilization doze (simple 1:1, doble 1:4 and quadrupled 1:8).

To determine the intracellular inorganic nitrate and phosphate in the sporophyte tissue, hot water extracts of dried kelp powder were prepared.

Intracellular nitrate was measured by weighing out around 10 mg dried kelp powder in Mettler Toledo UMT2 on a cover glass, and then transferred to glass test tubes with 4ml of distilled water. The tubes were boiled for 30 minutes with a marble placed on the top of the tube to avoid evaporation. After boiling the tubes were cooled down and filtered with a polysulfone syringe with a 0.45 μm filter to remove kelp particles from the concentrate. The samples from the sporophytes sampled right after every fertilization (Fertilized-FER) was diluted with 1:20 distilled water, due to high nutrient content.

To analyze the intracellular phosphorous, around 15mg of the dried powder were weighted out onto cover glass in the Mettler Toledo UMT2 and mixed with 4 ml 10Mm TrisHCl buffer (pH 7.0) in glass test tubes. The concentrate was boiled for 60 minutes with marble on top, cooled down, filtered (0.45 μm) and diluted 1:14 with distilled water.

The concentration of nitrate and phosphate in water and in the sporophyte tissue, were determined in an auto analyzer (Flow Solution IV System O.I Analytical Auto analyzer) according to Norwegian standard 4745. The output from the auto analyzer was given in $\mu\text{g L}^{-1}$ and Equation 2.1 and 2.2 were used to covert the values to $\mu\text{g NO}_3\text{-N mg}^{-1}\text{DW}$ and $\mu\text{g PO}_4\text{-P mg}^{-1}\text{DW}$ for the sporophyte tissue,

$$2.1 \quad \frac{\mu\text{g NO}_3 \text{ L}^{-1} * D * L}{\text{mg DW}} = \mu\text{g NO}_3 \text{ mg}^{-1}\text{DW}$$

$$2.2 \quad \frac{\mu\text{g PO}_4 \text{ L}^{-1} * D * E}{\text{mg DW}} = \mu\text{g PO}_4 \text{ mg}^{-1}\text{DW}$$

where, $\mu\text{g NO}_3 \text{ L}^{-1}$ and $\mu\text{g PO}_4 \text{ L}^{-1}$ were the output from the auto analyzer, D is the dilution, L is the extraction volume in liter and mg DW is the dry weight of the sample.

2.3.2 Total carbon and nitrogen

Particulate organic carbon and nitrogen (POC and PON) in the seawater in the basin were collected on GF-filters by filtering 500ml water in the filtration apparatus with 1 cm opening. After being stored in the freezer (-20°C), the part of the filter without particulate material on were cut off and the remaining filters were folded and placed in 5x9 mm tin capsules.

About 3 mg of the dry kelp powder samples were weighed out and placed into 5x9 mm tin capsules to determine the intracellular total carbon and nitrogen contents. The tin capsules with both the filters and the sporophyte powder were squeezed to a final form of a small ball to be placed in a well plate. The samples were dried at 60°C for 24h after formation of the balls to ensure the sample was complete dry. The total C and N in both the seawater and the sporophyte tissue were thereafter analyzed in an elemental analyzer (Elementar vario EL cube) using acetanilide (Sigma Aldrich 00401-5G) as external standard. The output from the elemental analyzer gave the $\mu\text{g C}$ and $\mu\text{g N}$ per sample. To get the $\mu\text{g mg}^{-1}\text{DW}$ in the sporophyte tissue, Equation 2.3 and 2.4 were used,

$$2.3 \quad \frac{\mu\text{g N}}{\text{mg DW}} = \mu\text{g N mg}^{-1}\text{DW}$$

$$2.4 \quad \frac{\mu\text{g C}}{\text{mg DW}} = \mu\text{g C mg}^{-1}\text{DW}$$

where mg DW is the dry weight of the sample, $\mu\text{g N}$ and $\mu\text{g C}$ is the output from the elemental analyzer.

2.3.3 Total phosphorus

Particulate organic phosphorous (POP) in the basin were measured in samples of 500ml seawater collected on GF-filters. The part of the filter without the particles were cut out and the remaining filter was placed in a in marked polyethylene scintillation vials. About 0.5 mg of the dried homogenized kelp powder sample was weighted in a Mettler Toledo UMT2 on a cover glass and put into marked polyethylene scintillation vials.

Both the filters and the dried kelp powder samples were further on treated with the same methodology. A volume of 10 ml of distilled water (H₂O), 0.1 ml 4M sulfuric acid (H₂SO₄) and 2 ml oxidizing reactant potassium peroxydisulfate (K₂S₂O₈) were added to the vials. The samples were gently shaken and heated in an autoclave at 120 °C for 30 minutes. After the samples had been cooled down the samples were filtered with a 0.45µm filter syringe to remove particle from the concentrate. The samples were then analyzed in the auto analyzer (Elementar vario EL cube) using acetanilide (Sigma Aldrich 00401-5G) as external standard. All the equipment used were acid washed by 0.5 M HCL before use. To calculate the internal P pr dry weight (µg mg⁻¹ DW) in the sporophytes Equation 2.5 were used,

$$2.5 \quad \frac{\mu g P L^{-1} * L}{mg DW} = \mu g P mg^{-1} DW$$

where, µg L⁻¹ is the output from the auto analyzer, L is the extraction volume in liter and DW is the dry weight of the sample.

2.3.4 Chlorophyll a

A total volume of 122.5 ml and 250 ml basin water were collected on GF-filters (2 cm opening). The volume depended on the amount of material in the water that was used to determine the Chl *a* concentration in the phytoplankton. Chl *a* in the sporophyte tissue was measured by cutting an approximately 1x1cm (around 0.05 g) fresh kelp piece. The filters or the fresh kelp piece were placed in glass tubes added 5ml methanol (CH₃OH) in a freezer (-20°C) for 24 h. After extraction, the samples were filtered into a new glass tube by using a syringe with 0.2 µm filter. The samples measured for the sporophytes were diluted with methanol, where the samples from the first two samplings were diluted 1:13 and 1:6.5 for the next twelve samplings. The seawater samples were not diluted. Exactly 1.6 ml of the diluted sample were measured in fluorometer (Turner Designs). The Chl *a* in the seawater basin samples were calculated by using equation (2.6) and the Chl *a* in the tissue was calculated by using Equation (2.7).

$$2.6 \quad \mu g Chl a L^{-1} = \frac{(FL - BL) \times f \times E \times 1000}{V \times 1000}$$

Where FL is the reading of the sample, BL is the blank sample (100%) methanol, *f* is the calibration factor (p.t. 0.47), *E* is the extraction volume in ml and *V* is the filtered volume in ml.

$$2.7 \quad \mu g Chl a mg^{-1} DW = \frac{(FL - BL) \times f \times E \times 1000}{mg \times DW \text{ ratio}}$$

Where *FL*, *BL*, *f* and *E* is the same as describes above. The *mg* is the fresh kelp piece in milligrams and the DW-rate was calculated by taking the mean of (wet weight/ dry weight) from each sampling (n=73), shown in Equation (2.8)

$$2.8 \quad DW \text{ ratio} = \frac{\text{dry weight}}{\text{fresh weight}}$$

2.3.5 PAM-fluorescence

An underwater Pulse amplitude modulated fluorometer (DIVING-PAM fluorometer) (Walz, Germany) was used to measure the photosynthetic activity in the lamina of *S. latissima* (Beer and Björk, 2000, Beer et al., 2000). The DIVING-PAM measure the chlorophyll fluorescence by flashing the lamina with high-intensity of light for 0.8 seconds when the sporophytes are dark-adapted (Beer and Björk, 2000). The Output (Fv/Fm) is a ratio that determines which amount of the photon from the light can be converted to electron transport in the photosystem II (PSII). The Fv/Fm is called the optimal quantum yield and shows the photosynthetic efficiency in the tissue where the light has been given (Beer and Björk, 2000, Kühl et al., 2001, Hanelt, 2018).

Three individuals from each treatment B:FER and B:CTL were collected in a Styrofoam box with seawater from the basin. The individual sporophytes were placed in a plastic box filled with seawater in a dark room with no sources of light. The DIVING-PAM fluorometer was calibrated by measuring the (Fv/Fm) in the seawater in the bucket and setting the fluorescence to zero. The DIVING-PAM fluorometer was then used to measure the photosynthetic activity in the sporophytes. The sporophytes were measured at three different sites on the lamina: the inner, mid and end part of the lamina.

2.3.6 Length measurements

The length of the sporophytes was analyzed by using Image J, where the laminated paper with reference were used to find the length.

To remove random variation and "noise" in the dataset an "smoothing" of the data was done, where the previous and the past measurements were included in each data point (Wood, 1982). The absolute growth rate was taken to look at the growth pr day, and the specific growth rate to look at the rate of increased length pr unit of length (Bhatia et al., 2015).

The absolute growth rate (cm day⁻¹) was calculated by using Equation 2.9

$$2.9 \quad \text{cm day}^{-1} = \frac{L_1 - L_0}{t}$$

The specific growth rate (μ) was calculated by using the Equation 2.10:

$$2.10 \quad \mu, \text{day}^{-1} = \frac{\left(\frac{L_1 - L_0}{t}\right)}{L_0}$$

Where L_1 and L_0 are the length in cm at the end and start of each measurement, and t is the time in days between each measurement.

2.3.7 Net uptake rate

The net uptake rate of nitrogen and phosphorus (V_x , g mg⁻¹ DW Day⁻¹) for both CTL and FER sporophytes from the end of February to beginning of July were calculated in Equation 2.11,

$$2.11 \quad V_x = \mu \times Q_x - \Delta Q_x$$

Where x is either Nitrogen (N) or Phosphorus (P), μ is the specific growth rate (μ , day⁻¹), Q_x is the total intracellular content of Nitrogen or phosphorus ($\mu\text{g mg}^{-1}$ DW) and ΔQ_x is the rate of change between the sampling dates (Droop, 1974).

2.3.1 Relationship between intracellular nutrient contents and the specific growth rate

The Droop-model shown in Equation 1.1 was used to examine the relationship between intracellular nutrient content and specific growth rate. The explanation of the different symbols used in the Equations are explained in Table 1.1. By multiplying the intracellular nutrients (Q_x) with Equation 1.1 the equation was transformed into linear equation. The transformation of Equation 1.1 is shown in Equation 2.13, and a linear function is shown in Equation 2.12.

$$2.12 \quad f(x) = ax + b$$

$$2.13 \quad \mu = \mu'_{max} \left(1 - \frac{Q_0}{Q}\right) \Leftrightarrow \mu * Q = \mu'_{max} Q - \mu'_{max} Q_0$$

The new linear equation were plotted and the growth coefficients μ'_{max} (a) is the slope of graph and $\mu'_{max} Q_0$ is the interception with y-axis (b). To find the minimum nutrient content for growth (Q_0) the intercept with the x-axis were done.

Based on the estimated Q_0 and μ'_{max} det Droop-model (Equation 1.1) were plotted with infinite Q-values, which resulted in a hyperbola growth curve. See section 3.7, Figure 3.10.

2.4 Statistics

Sigmaplot 14.0 were used to make the graphs and the statistical analysis. To see if there was a significant difference between the different treatments for the intracellular nutrient contents of N, P, C, Chl *a*, NO_3^- , PO_4^{3-} , an Shapiro-Wilk test were done to check for normality. For the data that was normally distributed an One Way Analysis of Variance (one way ANOVA) and student t-test were used, where ANOVA were used by comparing more than two treatments and Student t-test when two treatments were compared. For the data that were not normally distributed an All Pairwise Multiple Comparison Procedures (Dunn's Method) and Mann-Whitney Rank Sum Test were used. All Pairwise Multiple Comparison Procedures (Dunn's Method) were used to compare more than two treatments and the Mann-Whitney Rank Sum Test were used when comparing just two. The significance limit for the analysis was set to 0.05. The data presented in the graphs and tables include the mean with standard error (SE).

A linear regression was made in Sigmaplot 14.0 to assess the correlation between the specific growth rate (μ , day^{-1}) and total intracellular nitrogen Q_N and phosphorus Q_P (Q_x , $\mu g\ mg^{-1}\ DW$).

3 Results

3.1 Environmental conditions

The results for temperature and salinity are presented in Figure 3.1. The temperature in the seawater basin had a steady increase from 3.1 °C in the end of February to 16.5 °C in the beginning of July. The salinity in the basin was stable at 33.6 ± 0.07 ppt.

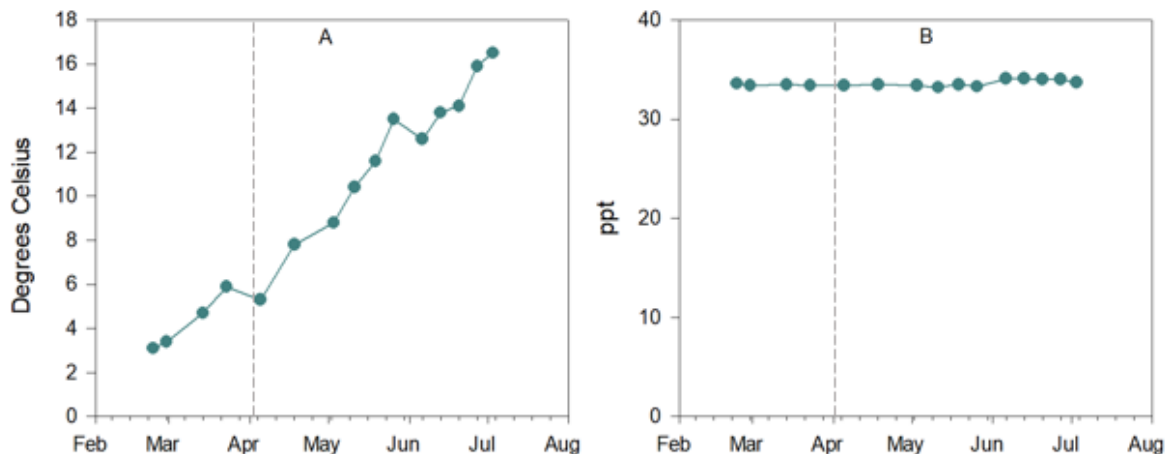


Figure 3.1: Environmental conditions in the seawater basin from the end of February to the beginning of July. A: The temperature (°C) in the basin and B: the salinity (ppt) in the basin. The gray dotted line symbolizes the demise of the spring bloom.

3.2 Water samples

Figure 3.2 shows the dissolved inorganic nutrients ($\text{NO}_3\text{-N}$ and $\text{PO}_4\text{-P}$), the total particulate organic compounds (PON, POC and POP) and the Chl *a* concentration in the seawater basin in the period from end of February to the beginning of July. The mean values of the particulate organic nutrients, inorganic nutrients, and Chl *a* are shown in Table 3.1, where the data is divided into the periods before and after the demise of the spring bloom, which was set to the 6th of April.

The concentration of $\text{NO}_3\text{-N}$ (nitrate) (Figure 3.2 A) in early February corresponded to the deep-water concentrations normally found in the north-east Atlantic coastal waters ($110\text{-}120 \mu\text{g NO}_3\text{-N L}^{-1}$) (Etter et al., 2016). The concentration dropped rapidly in March and stabilized after the phytoplankton spring bloom around 18th of April to a low value of around $10 \mu\text{g NO}_3\text{-N L}^{-1}$. Extracellular inorganic $\text{PO}_4\text{-P}$ (phosphate) (Figure 3.2 B) followed the same trend as for the nitrate, with values in early February within the concentrations seen in north-east Atlantic coastal deep waters ($18\text{-}20 \mu\text{g PO}_4\text{-P L}^{-1}$), decreasing to a low stable value ($\sim 1,5 \mu\text{g PO}_4\text{-P L}^{-1}$) in the spring and early summer (Etter et al., 2016).

The concentration of Chl *a* (Figure 3.2 C), which is a proxy for phytoplankton biomass, were low in late winter and had two peaks throughout the experiment. The first peak in late March represented the first spring bloom event in the basin. The second peak which started in May, increased to higher levels in June and leveled off towards July bringing the Chl *a* concentration to $1\text{-}4 \mu\text{g Chl } a \text{ L}^{-1}$. These values are normal in the Trondheim fjord and suggested that phytoplankton biomass reached a stable level in early June (Etter et al., 2016).

Particulate organic carbon, nitrogen, and phosphorus (Figure 1 D-F) followed the same pattern of variation as Chl *a* with low values in late winter and increased to a peak in June which leveled off in July.

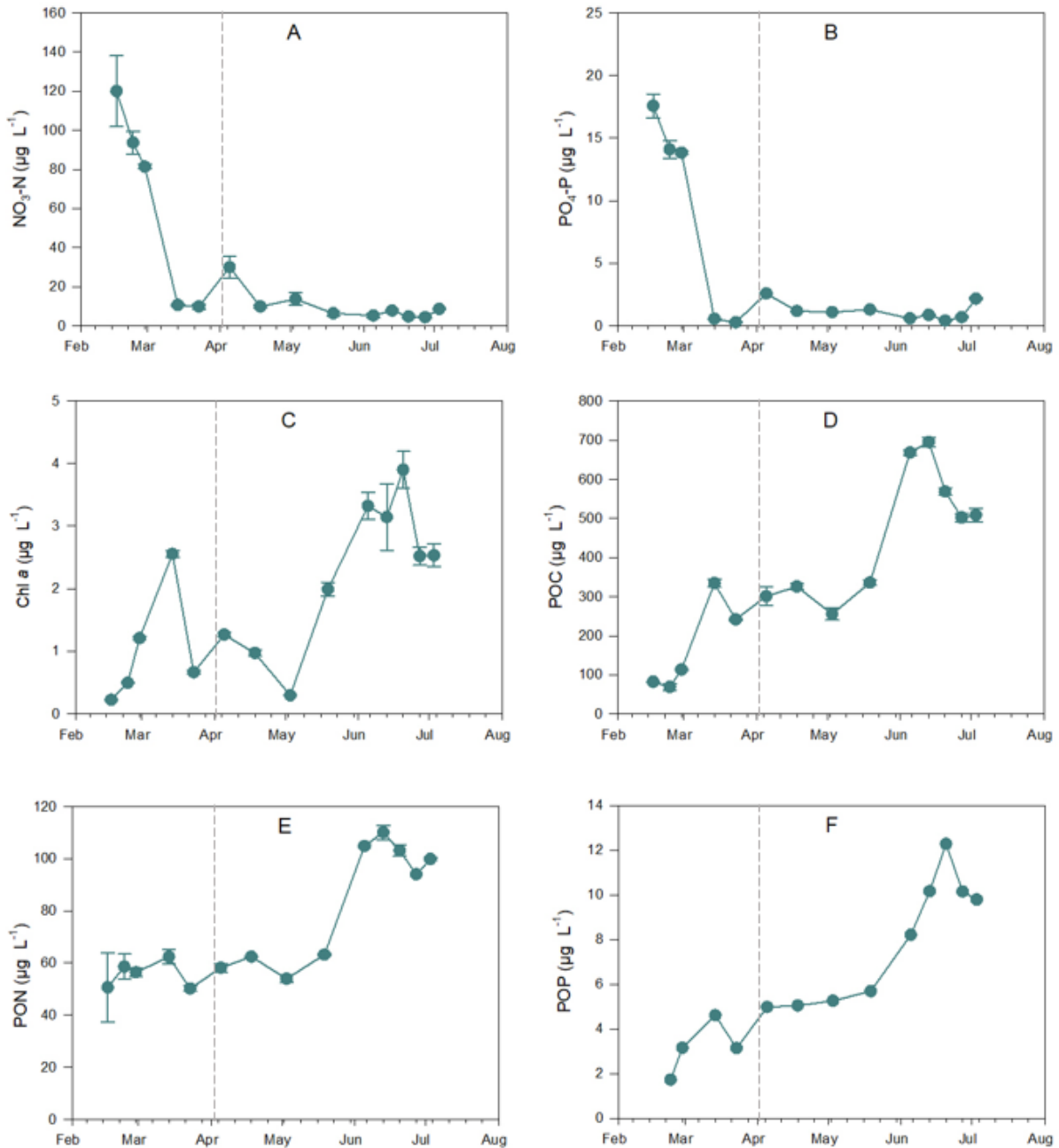


Figure 3.2: Nutrient and chlorophyll *a* concentration in the seawater basin in the period late February 2022 to early July 2022. A: Nitrate ($\mu\text{g NO}_3\text{-N L}^{-1}$), B: Phosphate ($\mu\text{g PO}_4\text{-P L}^{-1}$), C: chlorophyll *a* ($\mu\text{g L}^{-1}$), D: Particulate organic carbon ($\mu\text{g POC-C L}^{-1}$), E: Particulate organic nitrogen ($\mu\text{g PON-N L}^{-1}$) and F: Particulate organic phosphorus ($\mu\text{g POP-P L}^{-1}$), with standard error of the mean ($n=3$). The gray dotted line symbolizes the demise of the spring bloom.

Tabell 3.1: The mean values and the standard error of the mean of the total particulate organic compounds, extracellular concentrations of inorganic nutrients and chlorophyll *a* concentration of phytoplankton in the seawater basin in the period late February 2022 to early July 2022. The data is divided into before and after the spring bloom. The data is based on the graphs in Figure 3.2. (n=5-16 Before spring bloom, n=20-27 after spring bloom)

	Before spring bloom ($\mu\text{g L}^{-1}$)	After spring bloom ($\mu\text{g L}^{-1}$)
	Mean \pm SE	Mean \pm SE
NO ₃ -N	66.3 \pm 12.1	10.1 \pm 1.10
PO ₄ -P	9.79 \pm 1.92	1.16 \pm 0.13
Chl <i>a</i>	1.09 \pm 0.23	2.22 \pm 0.23
POC	168 \pm 34.5	462 \pm 35.7
PON	55.6 \pm 2.68	80.0 \pm 5.04
POP	3.16 \pm 0.59	7.95 \pm 0.92

Figure 3.3 shows the elemental ratios between PON:POC, POP:POC and PON:POP for particulate matter (<200 μm) dominated by phytoplankton in the basin from February to July, and Table 3.2 shows the mean concentrations of the ratios before and after the demise of the spring bloom.

The elemental ratio of PON:POC (Figure 3.3 A) showed very high values in the winter period (left panel) and values of around 180 $\mu\text{g mg}^{-1}$ after the demise of the spring bloom. After the demise of the spring bloom, the values corresponded with values earlier found for the period (Etter et al., 2016).

Also, the elemental ratio of POP:POC (Figure 3.3 B) showed high values in the winter period (left panel). The values decreased after the demise of the spring bloom and showed levels around 18 $\mu\text{g } \mu\text{g}^{-1}$.

The elemental ratio of PON:POP (Figure 3.3 C) showed values higher than the Redfield balance point for N and P limitation (Redfield, 1963) all through the experiment, but values before the spring bloom were particularly high (left panel).

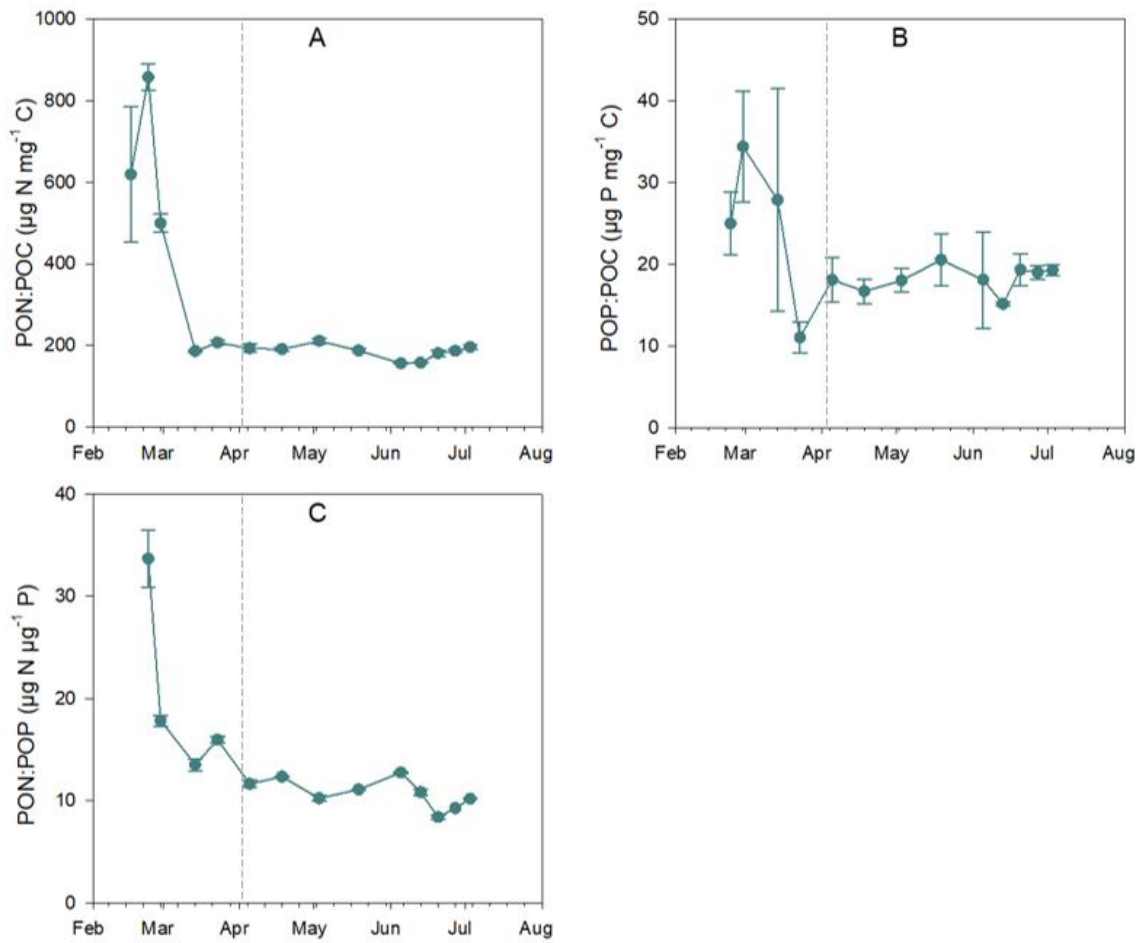


Figure 3.3: Elemental ratios of phytoplankton <200 μm in the seawater basin in the period late February 2022 to early July 2022. A: Nitrogen: Carbon ratio ($\mu\text{g N mg}^{-1} \text{C}$), B: Phosphorous: Carbon ratio ($\mu\text{g P mg}^{-1} \text{C}$) and C: Nitrogen: Phosphorous ratio ($\mu\text{g N } \mu\text{g}^{-1} \text{P}$) with standard error of the mean ($n=3$). The gray dotted line symbolizes the spring bloom.

Tabell 3.2: The mean elemental ratios of PON:POC, POP:POC and PON:POP in the seawater basin before and after the spring bloom with standard error of the mean ($n=10$ Before spring bloom and $n=18$ After spring bloom). The data is based on the graphs in Figure 3.3.

	Before the Spring bloom	After the spring bloom
	Mean \pm SE	Mean \pm SE
PON:POC ($\mu\text{g N: mg C}$)	474 \pm 88.3	185 \pm 4.25
POP:POC ($\mu\text{g P: mg C}$)	24.5 \pm 4.39	18.2 \pm 0.73
PON:POP ($\mu\text{g N: } \mu\text{g P}$)	20.3 \pm 3.04	10.8 \pm 0.33

3.3 Nutrient uptake in *Saccharina latissima* during fertilization

Table 3.3 shows the inorganic nitrate concentration and uptake in the fertilization tank during the eight fertilizations. These data are based on the water samples taken from the fertilization tank and the fertilization doze given to the tank.

The total concentration of nitrate ($\mu\text{g L}^{-1}$) added to the basin increased during the experiment. The concentration of the basin water pumped into the fertilization tank showed highest values in April-May. The end concentration of nitrate measured in the tank ($\mu\text{g L}^{-1}$) after the fertilization showed that the sporophytes (FER) of *Saccharina latissima* took up nitrate during the fertilization treatment, but that high nutrient concentration, close to or above deep-water concentrations normally, remained in the tank after the incubation (Etter et al., 2016). The nutrients taken up by the sporophytes per day increased when the fertilization doze increased. Nitrate were added in Redfield proportions (Redfield, 1963).

Tabell 3.3: The inorganic nitrate concentration and uptake in the fertilization tank during the eight fertilizations, with the total inorganic nitrate concentration ($\mu\text{g L}^{-1}$) added to the tank, the concentration in the tank water ($\mu\text{g L}^{-1}$) before the fertilization were added (basin water), the nutrients taken up from the tank during fertilization per day ($\mu\text{g L}^{-1} \text{ day}^{-1}$). Nitrate was added in Redfield proportions.

FER	Date	Total concentration added ($\mu\text{g NO}_3\text{-N L}^{-1}$)	Basin water ($\mu\text{g NO}_3\text{-N L}^{-1}$)	Fertilization tank, end concentration ($\mu\text{g NO}_3\text{-N L}^{-1}$)	Nutrients taken up ($\mu\text{g NO}_3\text{-N L}^{-1} \text{ day}^{-1}$)
1	6 th –7 th of April	280	-	156	124
2	19 th –20 th of April	280	9.47	122	167
3	4 th –5 th of May	280	18.5	194	104
4	20 th –21 st of May	560	0.00	311	249
5	5 th –7 th of June	1120	0.16	583	269
6	13 th – 15 th of June	1120	2.24	649	237
7	20 th – 22 nd of June	1120	7.23	527	300
8	27 th –29 th of June	1120	2.73	475	324

Table 3.4 shows the inorganic phosphate concentration and uptake in the fertilization tank during the eight fertilizations. These data are based on the water samples taken from the fertilization tank and the fertilization doze given to the tank.

The total concentration of phosphate ($\mu\text{g L}^{-1}$) added to the basin increased during the experiment. The end concentration of phosphate measured in the tank ($\mu\text{g L}^{-1}$) after the fertilization showed that the FER sporophytes of *S. latissima* took up phosphate during the fertilization treatment. High phosphate concentration, close to or higher than deep-water concentrations normally remained in the tank after the incubation (Etter et al., 2016). The phosphate taken up by the sporophytes per day increased when the fertilization doze increased. Nitrate was added in Redfield proportions (Redfield, 1963).

Tabell 3.4: The inorganic phosphate concentration and uptake in the fertilization tank during the eight fertilizations, with the total inorganic phosphate concentration ($\mu\text{g L}^{-1}$) added to the tank, the concentration in the tank water ($\mu\text{g L}^{-1}$) before the fertilization were added (basin water), the nutrients taken up from the tank during fertilization per day ($\mu\text{g L}^{-1} \text{ day}^{-1}$). Phosphate was added in Redfield proportions.

FER	Date	Total concentration added ($\mu\text{g PO}_4\text{-P L}^{-1}$)	Basin water ($\mu\text{g PO}_4\text{-P L}^{-1}$)	Fertilization tank, end concentration ($\mu\text{g PO}_4\text{-P L}^{-1}$)	Nutrients taken up ($\mu\text{g PO}_4\text{-P L}^{-1} \text{ day}^{-1}$)
1	6 th –7 th of April	38.7	-	25.5	13.2
2	19 th –20 th of April	38.7	0.97	21.4	18.3
3	4 th –5 th of May	38.7	1.37	32.8	7.27
4	20 th –21 st of May	77.4	1.23	56.6	22.0
5	5 th –7 th of June	155	0.48	85.3	70.0
6	13 th – 15 th of June	155	0.79	96.8	58.8
7	20 th – 22 nd of June	155	0.85	85.7	69.9
8	27 th –29 th of June	155	3.05	80.1	77.8

3.4 Elemental composition of the sporophytes

Figure 3.4 shows the inorganic intracellular nitrate and phosphate contents for the different treatments during experimental period. The mean values of nitrate and phosphate in the different treatments are shown in Table 3.5.

The content of nitrate (Figure 3.4 A) was far higher in the early stages before the spring bloom (left panel) with a maximum value of $7.31 \pm 0.70 \mu\text{g NO}_3\text{-N mg}^{-1} \text{ DW}$ in February. The values decreased rapidly to the end of March and remained stable after this. The content of nutrients after the demise of the spring bloom (right panel) showed low values in both CTL and FER sporophytes. The mean values of nitrate in CTL and FER sporophytes shown in Table 3.6 were similar and not statistically different ($P > 0.05$, Dunn's Method). The measurement done right after every fertilization (Fertilized-FER) showed higher content levels. This illustrates that the FER sporophytes took up nitrate during the fertilization treatment.

The intracellular inorganic phosphate (Figure 3.4 B) was also highest in the young sporophytes before the demise of the spring bloom (left panel), with a maximum content of $0.8 \pm 0.12 \mu\text{g PO}_4\text{-P mg}^{-1} \text{ DW}$. The content decreased and stabilized in the end of March. After the demise of the spring bloom (right panel) the phosphate content in the CTL and FER sporophytes was low and followed the same pattern of variation, where the content decreased in May and increased in June with the increased fertilization. The values for CTL and FER did not differ significantly ($P > 0.05$, Student t-test) until the last sampling in July where CTL sporophytes showed higher values than FER. The Fertilized-FER sporophytes showed significantly higher ($P < 0.05$, Student t-test) values than FER sporophytes in June.

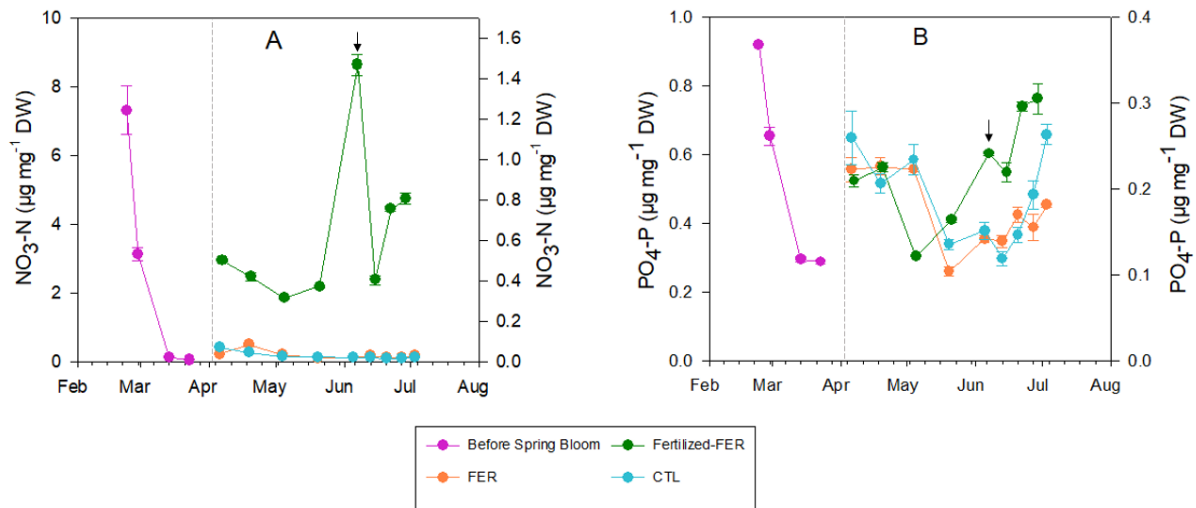


Figure 3.4: Inorganic nutrient contents in the tissue of *S. latissima* from the different treatments in the period from the end of February to the beginning of July. A: Nitrate ($\mu\text{g NO}_3\text{-N mg}^{-1}\text{ DW}$) and B: Phosphate ($\mu\text{g PO}_4\text{-P mg}^{-1}\text{ DW}$). Left panels: from late February until demise of spring bloom. Right panel: from demise of spring bloom till early July. The gray dotted line separates the graphs before and after the spring bloom and the scale of the y-axis. The arrow marks when the fertilization doze and incubation time increased. Error bars express standard error of the mean ($n=3$).

Figure 3.5 shows the total tissue contents of nitrogen, phosphorous and carbon and the intracellular Chl *a* content in the sporophytes during the experiment. Table 3.5 shows the mean values in the period before the spring bloom and the period from after the demise of the spring bloom (6th of April) when fertilization took place.

The total intracellular nitrogen (Q_N , Figure 3.5 A) showed highest content before the demise of the spring bloom (left panel) with the maximum at $23.7 \pm 0.26 \mu\text{g N mg}^{-1}\text{ DW}$. After the demise of the spring bloom (right panel), the N contents in CTL sporophytes decreased steadily from late April all through the experiment, while the FER sporophyte showed a beginning increase compared to CTL from mid-May, and a larger increase in June. The Fertilized-FER sporophytes showed higher N contents than in FER all through the experimental period.

The intracellular phosphorus content (Q_P , Figure 3.5 B) followed almost the same pattern of variation as the nitrogen, where in the left panel the highest values were found for the earliest stages and decreased to the demise of the spring bloom. The maximum value was 2.74 ± 0.05 . In the right panel, the three treatments showed no significant difference ($P>0.05$, Dunn's Method) until mid-June, where the values in CTL sporophytes decreased further, and the FER values increased. The Fertilized-FER did not show values higher than the FER until mid-May. Fertilized-FER showed values through significantly higher than the CTL and FER ($P<0.05$, Dunn's Method). The last measurements done in July is considered as a contamination for all three treatments.

For the intracellular carbon (Q_C , Figure 3.5 C) the carbon per dry matter values were higher in the period after the spring bloom (right panel) with a mean value of $232 \pm 2.50 \mu\text{g C mg}^{-1}\text{ DW}$ for all three treatments combined. The early stages before the spring bloom in the left panel were slightly lower than the content before the spring bloom in the left panel. The values for intracellular carbon in all treatments were quite stable throughout the whole

experiment, with no significant differences ($P > 0.05$, Dunn's Method) between the CTL, FER and Fertilized-FER.

The Chl *a* content in sporophyte tissue (Figure 3.5 D) followed the same pattern of variation as nitrogen and phosphorus, decreasing steadily till the demise of the spring bloom. The highest concentration was found in the winter (left panel) with a maximum value around $30 \mu\text{g Chl } a \text{ mg}^{-1} \text{ DW}$. After the demise of the spring bloom (left panel) the CTL sporophytes showed a decrease the content of Chl *a* throughout the experiment. The values for FER sporophytes were not significantly different ($P > 0.05$, Student t-test) from the CTL sporophytes until the beginning of June when the FER sporophytes increased their Chl *a* content rapidly.

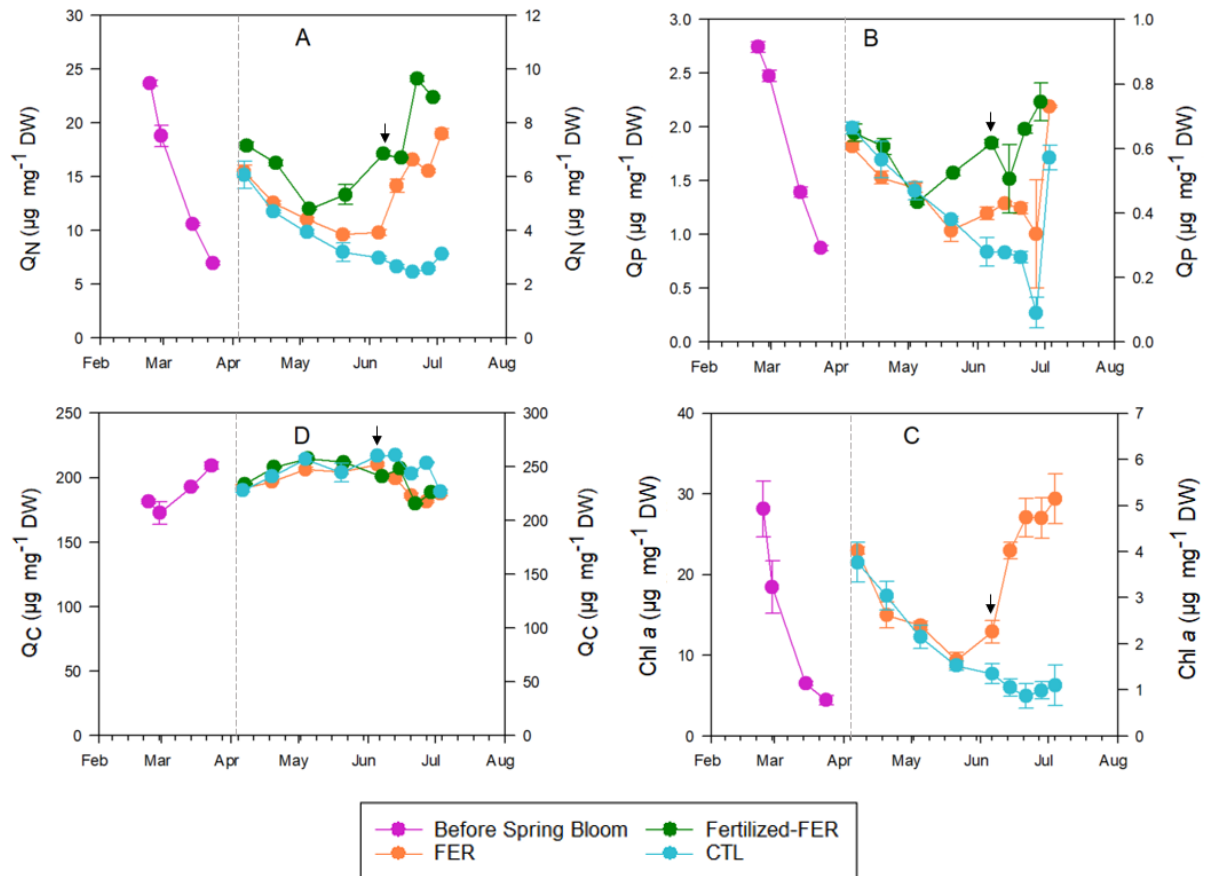


Figure 3.5: Total tissue contents of nutrients and chlorophyll *a* in the different treatments of *S. latissima* in the period from late February to beginning of July. A: Total intracellular nitrogen (Q_N , $\mu\text{g N mg}^{-1} \text{ DW}$), B: Total intracellular phosphorus (Q_P , $\mu\text{g P mg}^{-1} \text{ DW}$), C: Total intracellular carbon (Q_C , $\mu\text{g C mg}^{-1} \text{ DW}$) and D: Chlorophyll *a* ($\mu\text{g Chl } a \text{ mg}^{-1} \text{ DW}$). Left panels: from late February until demise of spring bloom. Right panel: from demise of spring bloom till early July. The gray dotted line separates the graphs before and after the spring bloom and the scale of the y-axis. The arrow marks where the fertilization doze and incubation time increased. Error bars express standard error of the mean ($n=3$).

Tabell 3.5: The mean values and the standard error of the mean for the total tissue contents of nutrients (Q_N , Q_P and Q_C), inorganic nutrients (NO_3 -N and PO_4 -P) and chlorophyll *a* in the different treatments of *S. latissima* in the period from late February to beginning of July. (n=14-27). The data is based on the graphs in Figure 3.4 and 3.5.

	Mean \pm SE Before spring bloom ($\mu\text{g mg}^{-1}$ DW)	Mean \pm SE FER ($\mu\text{g mg}^{-1}$ DW)	Mean \pm SE Fertilized-FER ($\mu\text{g mg}^{-1}$ DW)	Mean \pm SE CTL ($\mu\text{g mg}^{-1}$ DW)
Q_N	15.0 \pm 1.72	5.50 \pm 0.24	6.99 \pm 0.32	3.42 \pm 0.21
Q_P	18.7 \pm 0.20	0.47 \pm 0.03	0.59 \pm 0.02	0.39 \pm 0.15
Q_C	189 \pm 0.71	235 \pm 2.28	241 \pm 2.85	247 \pm 2.53
Chl <i>a</i>	14.4 \pm 2.29	3.51 \pm 0.25	-	1.76 \pm 0.21
NO_3 -N	1.98 \pm 0.71	0.032 \pm 0.0039	0.51 \pm 0.04	0.026 \pm 0.003
PO_4 -P	0.40 \pm 0.037	0.17 \pm 0.0083	0.22 \pm 0.012	0.19 \pm 0.011

Figure 3.6 shows the elemental ratios of N:C, P:C and N:C in kelp tissue in the different treatments from late February to early July 2022. Table 3.6 shows the mean value of the ratios in the different treatments with the standard error of the mean.

The N:C ratio (Figure 3.6 A) followed the same pattern of variation as the intracellular nitrogen content per dry matter (Figure 3.5 A), where the highest values were found in the winter and an almost linearly decrease to the demise of the spring bloom (left panel). In the right panel, the values of the CTL sporophytes decreased through the whole experiment, while the ratio of FER sporophytes decreased until the beginning of June where the nitrogen content increased rapidly. The Fertilized-FER had values higher than the FER sporophytes, revealing that the sporophytes took up nitrogen during the fertilization treatment.

The P:C ratio (Figure 3.6 B) also correspond to the intracellular phosphorous content per dry matter shown in Figure 3.6 B, where the values in the left panel are higher than in the right panel. In the right panel the CTL sporophytes decreased throughout the whole experiment and there was no significant difference ($P > 0.05$, ANOVA) between the three treatments until the beginning of June. In June the FER sporophytes increased their P:C ratios, and the Fertilized-FER sporophytes showed higher values than the FER. The values in the last data point (3rd of July) suggested that there was a phosphorus contamination.

The N:P ratio (Figure 3.6 C) of sporophyte tissue showed the highest values before the demise of the spring bloom (left panel). In the right panel the CTL, FER and Fertilized-FER showed stabile N:P ratio with no significant difference ($P > 0.05$, Dunn's Method) was found until the beginning of June. In June the CTL sporophytes showed a slight decrease in N:P ratio, while the FER sporophytes increased values. The high values in the CTL and the low values in the Fertilized-FER in July, supported that there likely had been a phosphorus contamination in the actual sample.

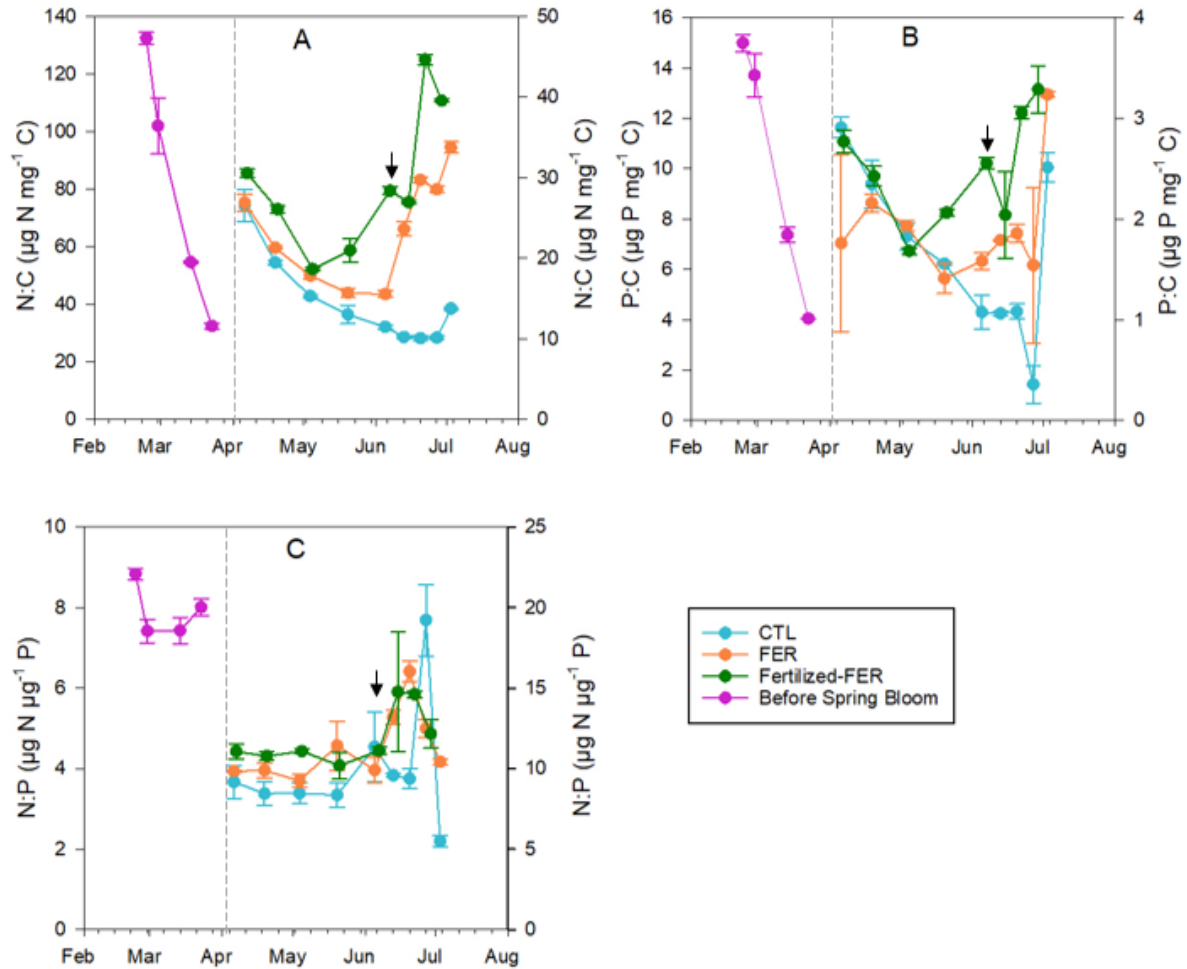


Figure 3.6: The elemental ratios in the tissue of *S. latissima*. A: N:C ($\mu\text{g N } \mu\text{g}^{-1} \text{C}$), B: P:C ($\mu\text{g P } \mu\text{g}^{-1} \text{C}$) and C: N:P ($\mu\text{g N } \mu\text{g}^{-1} \text{P}$). Left panels: from late February until demise of spring bloom. Right panel: from demise of spring bloom till early July. The gray dotted line separates the graphs before and after the spring bloom and the scale of the y-axis. The arrow marks where the fertilization dose and incubation time. Error bars express standard error of the mean ($n=3$). The data are based on the values for Q_N , Q_P and Q_C shown in figure 3.5 A-C and Table 3.5.

Tabell 3.6: The mean values and the standard error of the mean for the elemental ratios of N:C ($\mu\text{g N } \mu\text{g}^{-1} \text{C}$), P:C ($\mu\text{g P } \mu\text{g}^{-1} \text{C}$) and N:P ($\mu\text{g N } \mu\text{g}^{-1} \text{P}$) in the different treatments of *S. latissima* in the period from late February to beginning of July. The data is based on the graphs in Figure 3.6. ($n=12$ before the spring bloom and $n=24$ for CTL, FER and Fertilized-FER)

	Mean \pm SE Before spring bloom	Mean \pm SE FER	Mean \pm SE Fertilized-FER	Mean \pm SE CTL	Unit
N:C	80.4 \pm 12.0	23.6 \pm 1.22	29.5 \pm 1.62	14.0 \pm 0.93	$\mu\text{g N } \mu\text{g}^{-1} \text{C}$
P:C	10.0 \pm 1.37	1.92 \pm 0.15	2.49 \pm 0.11	1.59 \pm 0.16	$\mu\text{g P } \mu\text{g}^{-1} \text{C}$
N:P	7.92 \pm 0.21	11.4 \pm 0.48	12.0 \pm 0.51	9.60 \pm 0.72	$\mu\text{g N } \mu\text{g}^{-1} \text{P}$

3.5 Sporophyte growth

Figure 3.7 shows the increase in length of sporophytes (cm) from the end of February to the beginning of July. Before the demise of the spring bloom (left panel) the sporophytes had a stable almost linear increase in length. After the demise of the spring bloom (right panel) from April to the end of May the sporophytes in CTL and FER had a continuous increase in length with no significant difference ($P > 0.05$, Mann-Whitney Rank Sum Test). From June until the end of the experiment, the CTL sporophytes decreased in length while the FER sporophytes continued the steady increase in length.

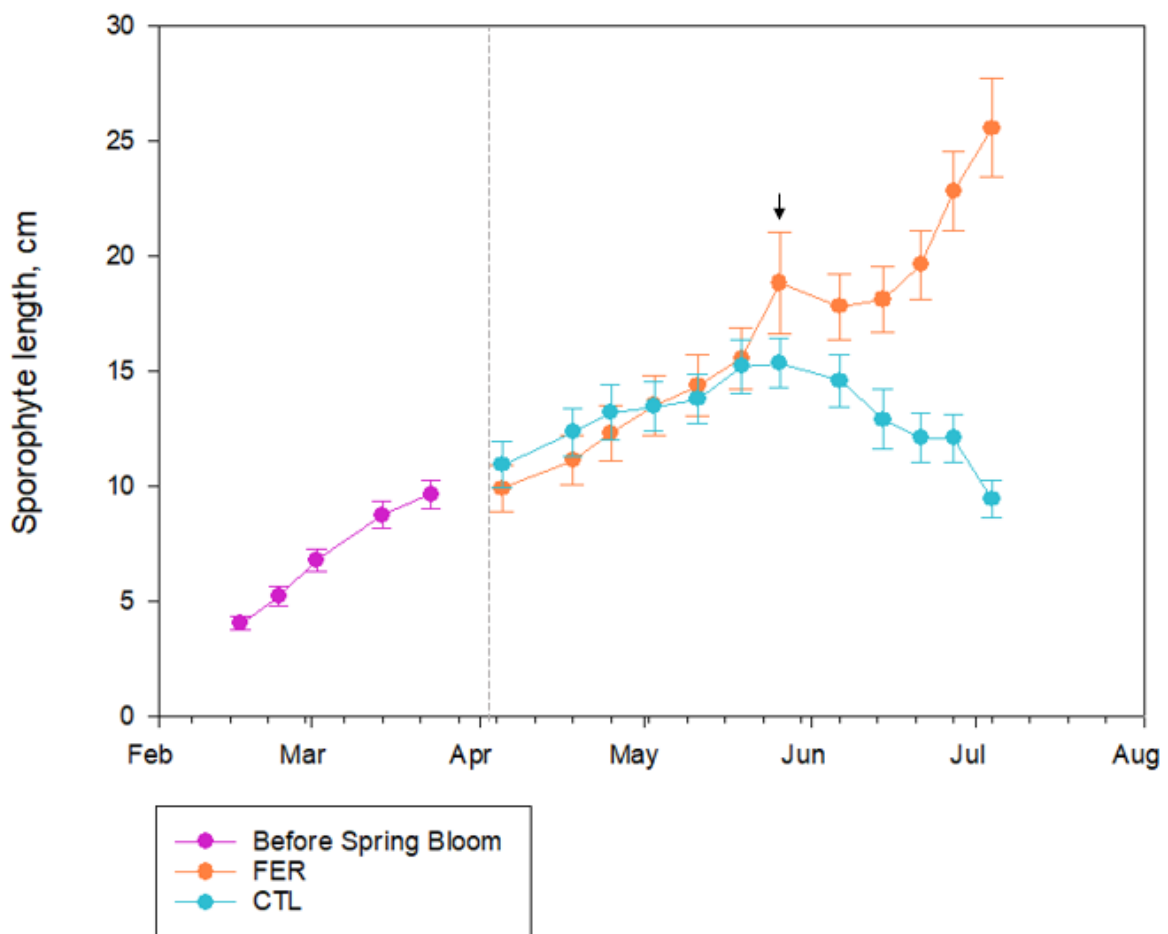


Figure 3.7: The length (cm) of the sporophytes before the spring bloom, and for FER and CTL treatment in the period from late February to early July. Left panels: from late February until demise of spring bloom. Right panel: from demise of spring bloom till early July. The gray dotted line separates the graphs before and after the spring bloom. Error bars express standard error of the mean ($n=81$ for CTL and 103 for FER) with data smoothing. The arrow marks when the fertilization doze and incubation time increased (Table 2.1).

Figure 3.8 shows the absolute (cm day^{-1} , Figure 3.8A) and the specific growth rate (day^{-1} , Figure 3.8B) of *S. latissima* before the demise of the spring bloom and the CTL and FER sporophytes after the demise of the spring bloom. Before the demise of the spring bloom

(left panel) the sporophytes showed a slight decrease in the absolute growth rate (Figure 3.8A) from highest growth rate in the winter. In the right panel after the demise of the spring bloom, the CTL sporophytes showed a continuous decrease with an absolute growth rate below zero. The FER sporophytes showed an increased absolute growth rate from April to the end of the experiment, with a rapid increase and high values beyond mid-June and remained positive all through.

The same pattern of variation is shown for the specific growth rate (Figure 3.8B), where the highest growth rate was found in February, and it decreased until the demise of the spring bloom (left panel). After the demise of the spring bloom the CTL sporophytes showed a continuous decrease through the whole experiment, with values below zero. The specific growth rate of FER sporophytes became gradually higher than those of CTL sporophytes from late April-early May, before increasing further on in June. The specific growth rate of the sporophytes was throughout higher for the early developmental stages, before the demise of the spring bloom, than after the bloom.

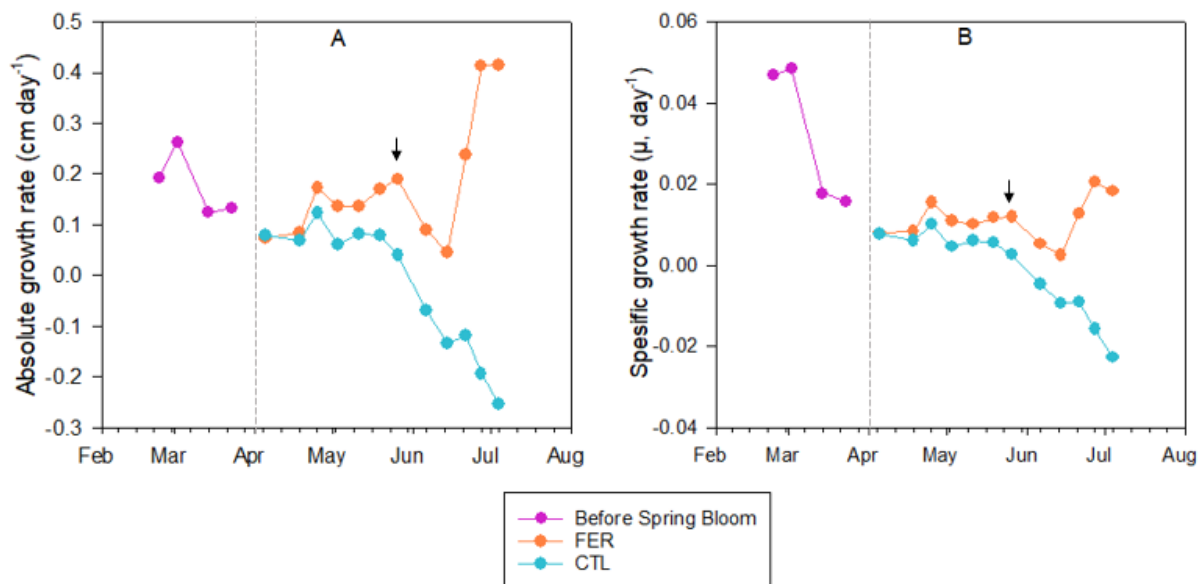


Figure 3.8: The absolute and specific growth rates of the sporophytes from the end of February 2022 to the beginning of July 2022. A: Absolute growth rate (cm day^{-1}) and B: Specific growth rate (μ, day^{-1}). Left panels: from late February until demise of spring bloom. Right panel: from demise of spring bloom till early July. The gray dotted line separates the graphs before and after the spring bloom and the arrow marks when the fertilization doze and incubation time increased.

3.6 Net uptake of nutrients

Figure 3.9 shows the net uptake rate for nitrogen (V_N) and phosphorus (V_P) during the experimental period, based on Equation 2.11. Table 3.7 shows the average mean net uptake and the change in internal nutrient content (ΔQ) for before the spring bloom and for the CTL and FER sporophytes.

The net N uptake rate for nitrogen (Figure 3.9A) before the spring bloom (left panel) showed decreasing values from February to the demise of the spring bloom in early April,

with a low value the 2nd of March. In the right panel, the net uptake of nitrogen in the CTL sporophytes were relatively constant throughout the experiment with values below zero. The FER sporophytes showed a stable increase in net N uptake with values over zero. The mean ΔQ_N value for CTL sporophytes was not significantly different from zero ($P > 0.05$, student t-test). The ΔQ_N value for FER was on average significantly different from zero ($P < 0.05$, student t-test). The negative value of V_N and ΔQ_N in CTL suggested that the sporophytes used internal nitrogen resources for growth, while the FER sporophytes took up nitrogen from the fertilization throughout the whole experiment.

Almost the same pattern of variation is shown for the net uptake of phosphorous (Figure 3.9B). In the right panel before the demise of the spring bloom, the sporophytes had highest net uptake in February and the uptake decreased rapidly until the demise of the spring bloom, with a low value the 2nd of March. After det demise of the spring bloom (right panel) the CTL sporophytes showed stable values around and below zero with a decrease in the end of June. The FER sporophytes showed also values around zero, with a slight increase in June and a rapid increase in the end of June. The mean ΔQ_P value for CTL sporophytes was not significantly different from zero ($P > 0.05$, student t-test). The ΔQ_P value for the FER sporophytes was also on average not significantly different from zero ($P > 0.05$, student t-test). The negative value of V_P and ΔQ_P in June suggested that the CTL sporophytes used internal stored nutrients for growth. The positive net P uptake in the FER sporophytes suggested that they took up nutrients from the water in June. The values in the last data point (3rd of July) suggested that there was a phosphorus contamination.

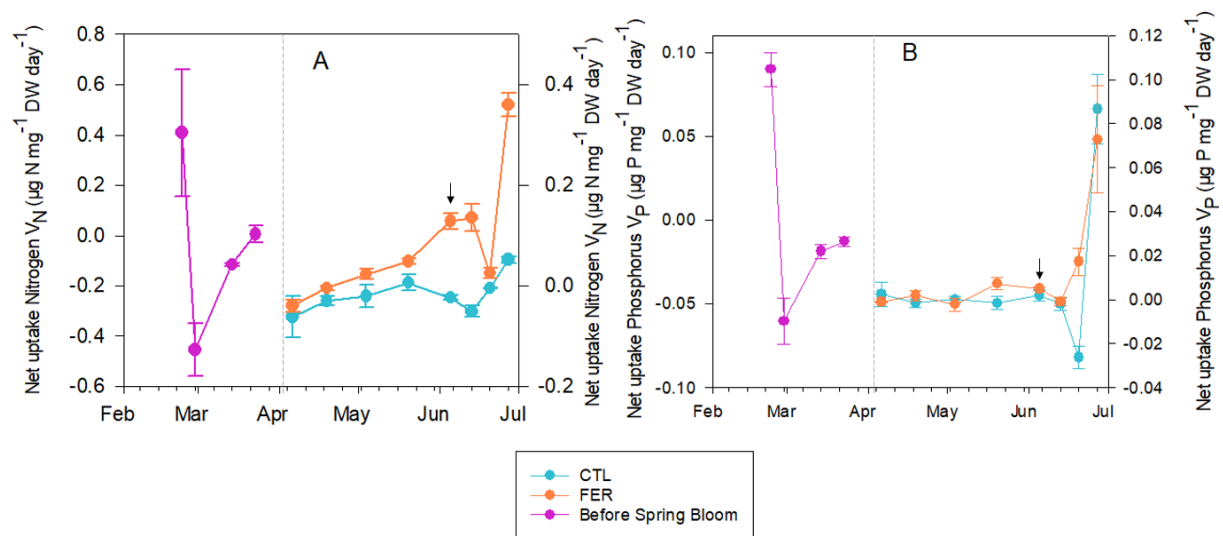


Figure 3.9: The net uptake of nutrients during the experiment. A: net uptake of nitrogen (V_N , $\mu\text{g N mg}^{-1} \text{ DW day}^{-1}$) and B: net uptake of phosphorus (V_P , $\mu\text{g P mg}^{-1} \text{ DW day}^{-1}$). Left panels: from late February until demise of spring bloom. Right panel: from demise of spring bloom till early July. The gray dotted line separates the graphs before and after the spring bloom and the scale of the y-axis. The arrow marks when the fertilization doze and incubation time increased. Error bars express standard error of the mean ($n=3$).

Tabell 3.7: The mean values and the standard error of the mean for the net uptake of nitrogen ($\mu\text{g N mg}^{-1} \text{DW day}^{-1}$) and phosphorus ($\mu\text{g P mg}^{-1} \text{DW day}^{-1}$) and the ΔQ in the different treatments of *S. latissima* in the period from late February to beginning of July. The data is based on the graphs in Figure 3.9 and is calculated with Equation 2.11 ($n=12$ and 24).

	Mean \pm SE Before spring bloom	Mean \pm SE FER	Mean \pm SE CTL	Unit
V_N	-0.039 ± 0.12	0.084 ± 0.025	0.015 ± 0.008	$\mu\text{g N mg}^{-1} \text{DW day}^{-1}$
ΔQ_N	0.61 ± 0.13	0.17 ± 0.089	0.017 ± 0.077	$\mu\text{g N mg}^{-1} \text{DW day}^{-1}$
V_P	-0.0005 ± 0.017	0.013 ± 0.0015	0.0046 ± 0.0022	$\mu\text{g P mg}^{-1} \text{DW day}^{-1}$
ΔQ_P	0.072 ± 0.017	-0.0055 ± 0.0061	-0.0039 ± 0.0055	$\mu\text{g P mg}^{-1} \text{DW day}^{-1}$

3.7 Relationship between intracellular nutrient contents and specific growth rate

Figure 3.10 (A, B) show the specific growth rate of the sporophytes as function of intracellular N (Q_N , Figure 3.10 A) and P (Q_P , Figure 3.10 B). There was a non-linear positive relationship between the specific growth rate in both Q_N and Q_P . Both growth rate and internal nutrient contents were highest in early developmental stages of the algae, values found before the demise of the spring bloom.

The pattern of variation in Figure 3.10 A, B is similar to what is regularly found in microalgae and is normally described by the Droop-model that express specific growth rate as a function of intracellular limiting nutrient contents (Droop, 1974). Equation 1.1 and Table 1.1 describes the Droop-model for both nitrogen (Q_N) and phosphorous (Q_P). The coefficients of the model can be estimated using linear regression of the transformation $Q_x \times \mu$ versus Q_x (x is N or P) (Equation 2.13). The growth coefficients μ'_{\max} is the slope of graph and Q_{0x} is the interception with y -axis (Figure 3.10 C and D).

Both curves of Figure 3.10 C and D are accepted as linear, indicating a proper fit of the model to the data (R^2 value close to 1 and $P < 0.0001$), and the calculated coefficients μ'_{\max} , Q_{0N} and Q_{0P} with confidence limits are shown in Table 3.8. The curves describing the Droop model for estimated μ'_{\max} and Q_0 values are shown for N and P in Figure 3.10 A and B, respectively. The variability in data is well within the normal for microalgae, and the model was found to describe the data quite well (Droop, 1974).

The highest growth rate and internal nutrient content were measured in the early stages of the sporophytes, in late February and early March. The average value of these datapoints is assumed to express the maximum specific growth rate of the algae (μ_{\max}) and the maximum internal nitrogen and phosphorous content which allow this growth rate (Q_m) can be extrapolated from the μ_{\max} value. The estimated datapoint for Q_m and (μ_{\max}) with confidence limits are shown in red in Figure 3.10 A-B and the values of Q_m and μ_{\max} are presented in Table 3.8.

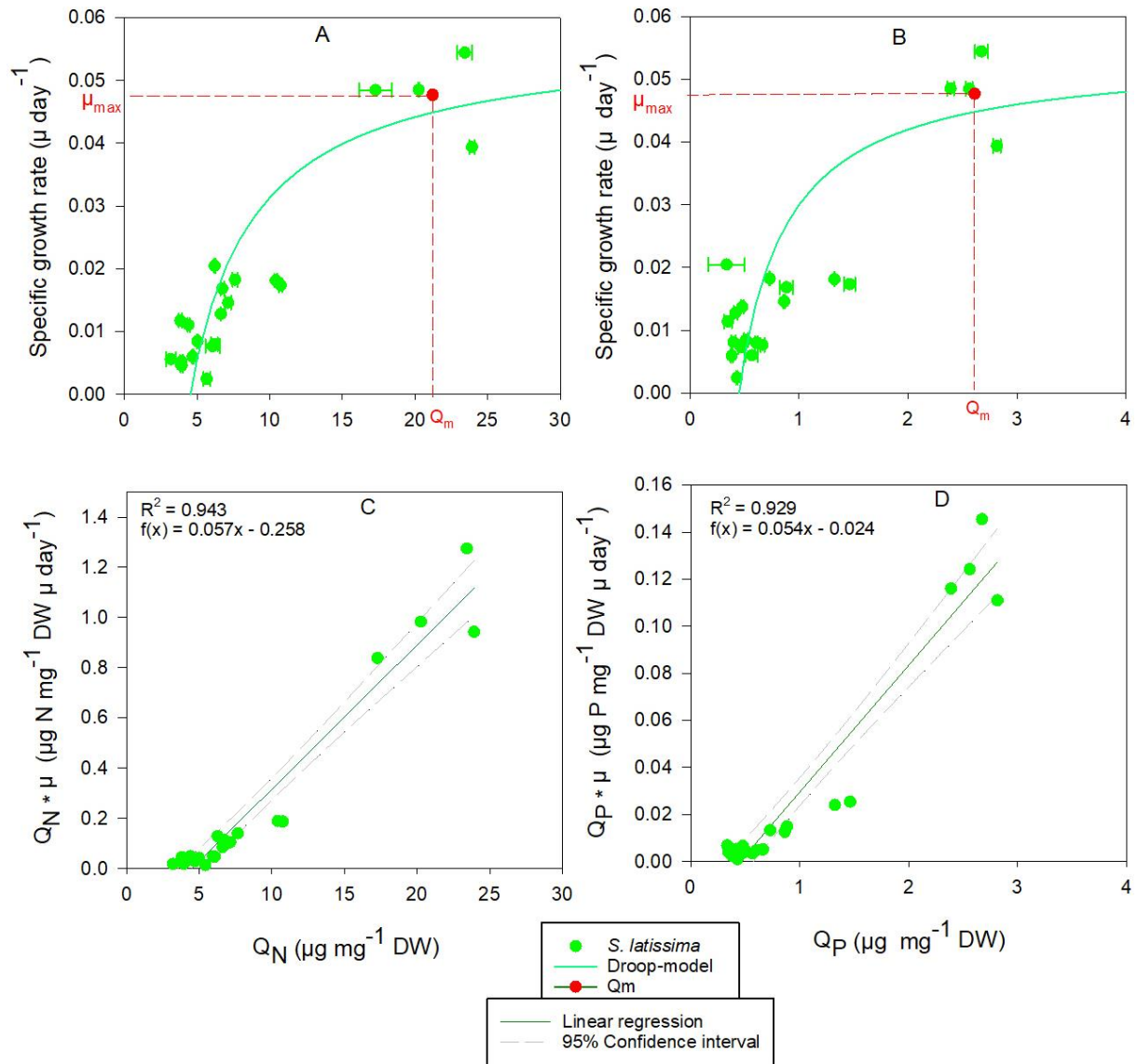


Figure 3.10: The Droop-model. A-B: The specific growth rate of *S. latissima* sporophytes (μ , day^{-1}) as a function of the intracellular nutrients contents (Q_x), with the Q_m and μ_{\max} marked in red and the hyperbola Droop-graph in green. A: intracellular nitrogen contents (Q_N , $\mu\text{g N mg}^{-1}\text{ DW}$) ad B: Intracellular phosphorous content (Q_P , $\mu\text{g P mg}^{-1}\text{ DW}$). The error bars are the standard error of mean (SE, $n=3$). C-D: The transformation done to find the Droop-equation, which was the intracellular nutrient content of *S. latissima* (Q_x) times the specific growth rate (μ , day^{-1}) as a function of the intracellular nutrient contents (Q_x), with linear regression and the 95% confidence interval marked in green dotted line. C: is for the intracellular N contents (Q_N , $\mu\text{g N mg}^{-1}\text{ DW}$) and B: is for the intracellular P content (Q_P , $\mu\text{g P mg}^{-1}\text{ DW}$). The data points are all the positive values measured of *S. latissima* from the different treatment combined.

Tabell 3.8: The values of Q_0 , μ'_{\max} , Q_m and μ_{\max} for both the Q_N and Q_P , based the Droop-model in Figure 3.10. The values were calculated form Equation 1.1 and 2.13. (mean \pm SE, $n=3$ and $n=2$ (Q_0 , μ'_{\max}) and $n=8$ (Q_m , μ_{\max}))

	$Q_N \pm \text{SE}$	$Q_P \pm \text{SE}$	Unit
Q_0	4.5 ± 0.42	0.44 ± 0.06	$(\mu\text{g mg}^{-1}\text{ DW})$
μ'_{\max}	0.057 ± 0.003	0.054 ± 0.003	(Day^{-1})
Q_m	21.2 ± 1.04	2.61 ± 0.089	$(\mu\text{g mg}^{-1}\text{ DW})$
μ_{\max}	0.048 ± 0.0031	0.048 ± 0.0031	(Day^{-1})

3.8 Sporophyte health

Figure 3.8 shows the PAM-fluorescence for *S. latissima* of CTL and FER sporophytes from the beginning of June to the beginning of July, which is the period when the highest fertilization doze were given to the FER sporophytes. A general pattern of the photosynthetic efficiency along the lamina was observed in both treatments. The highest values measured was measured close to the stem of the sporophyte and decreased to the end of the lamina. This pattern of variation was seen in sectors of the lamina (inner part of the lamina: A,a) which showed the highest values, followed by (middle part of the lamina: B,b), and (end of the lamina: C,c) showing the lowest values in each treatment and sampling-day.

The results showed a steady phase with values close to 0.6 Fv/Fm in the FER sporophytes from 13th of June. The CTL sporophytes showed values lower than the FER and in some cases zero, which demonstrated a big deterioration of the end of the lamina.

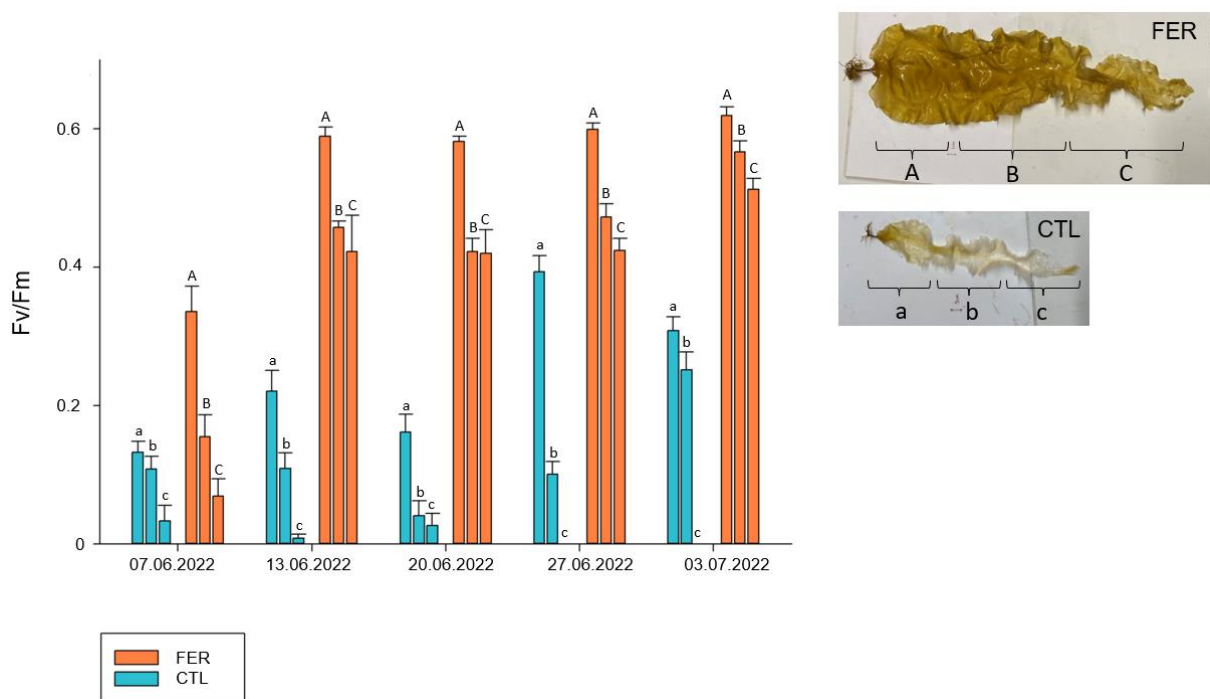


Figure 3.11: The PAM-fluorescence (Fv/Fm) in sporophytes from FER and the CTL sporophytes in June 2022. The orange bars and the upper picture (ABC) are the FER and the blue bars, and the bottom picture (abc) are the CTL. The sporophytes were divided into three sections where the measurement were done upper part of the lamina (A,a), middle part of the lamina (B,b) and the tip of the lamina (C,c) part of the lamina as shown in the pictures. Error bars express standard error of the mean (n=9).

4 Discussion

The aim of this thesis was to investigate if there is a competition over inorganic nutrients between *Saccharina latissima* and phytoplankton communities, and if the competitive ability, growth, and nutritional state of *S. latissima* increased by being exposed to short-term dose of fertilization. The results of this study showed that the phytoplankton community was not negatively affected by the *S. latissima*. The young sporophytes had the highest nutrient storage, that was used for growth in the spring. By comparing the nutritional state and growth rate of the phytoplankton with the control sporophytes (CTL) the result suggested that there is a competition in nutrient uptake, and that phytoplankton are favored. The fertilization treatment increased the nutritional state and growth of the FER sporophytes suggesting that a fertilization treatment induced the competitive ability. A positive correlation between specific growth rate and intracellular nutrient content in *S. latissima* were also established and showed that the young sporophytes in the winter period have the highest nutrient content and growth rate.

4.1 Physical conditions

Seawater quality and physiochemical properties are essential for seaweed to grow in an optimal manner (Harrison and Hurd, 2001, Hurd et al., 2014). The salinity values of the basin were stable at 33.6 ± 0.07 ppt which was slightly higher than other values reported from Trønderlag and the Trondheimsfjord (Etter et al., 2016, Hegseth and Sakshaug, 1983). Variation in salinity can be explained by the amount of fresh water supply and circulation, which in our experiment were low, due to no fresh water runoff in the basin and little rainfall during the experimental period (Sarmiento and Gruber, 2006).

The temperature showed a steady increase from 3.1-16.5°C from the end of February to beginning of July, which corresponds to the temperature level earlier measured in the Trondheimsfjord right outside Trondheim Biological Station from February to July (-0.9-16°C) (Hegseth and Sakshaug, 1983). Temperature changes during the season, but can also be affected by several other factors, such as freshwater runoffs, currents, and other physical factors (Sarmiento and Gruber, 2006). However, the values show normal seasonal change in temperature and normal stable salinity levels. By considering the optimal temperature (10-15°C) and salinity (27-33 ppt) for *S. latissima*, the measured salinity and temperature in May-June corresponds with the optimal values for *S. latissima*, suggesting, that the growth and uptake were not much restricted by the temperature (Bolton and Lüning, 1982, Nielsen et al., 2016).

There is also a seasonality of light, temperature and dissolved nutrient concentration in temperate coastal and fjord waters (Rey, 2004). During the winter period light is the limiting factor, while in the summer period nutrients becomes the normal limiting factor after the spring bloom in temperate waters (Rey, 2004). In this experiment the inorganic dissolved nitrate and phosphate decreased rapidly from February with around $120 \mu\text{g NO}_3\text{-N L}^{-1}$ and $18 \mu\text{g PO}_4\text{-P L}^{-1}$ to the mid-end of March with around $10 \mu\text{g NO}_3\text{-N L}^{-1}$ and $1 \mu\text{g PO}_4\text{-P L}^{-1}$. At the same time as the inorganic concentration of nutrients decreased, the phytoplankton had a peak in Chl *a* concentration. The first spring bloom thereby took place in the basin around the end of March, which is slightly earlier than what is normal, which is early-mid April (Haug et al., 1973, Deininger et al., 2022, Sakshaug and Mykkestad, 1973). However, based on the combination of increased light and temperature, an earlier growth of phytoplankton was observed in the basin, which caused the early peak in Chl *a*.

A spring bloom in late March have been observed in other studies (Etter et al., 2016, Sakshaug and Mykkestad, 1973).

4.2 Environmental state of phytoplankton

Phytoplankton are key organisms in the marine ecosystem, thus, any perturbation could affect the natural equilibrium among components of the ecosystem (Semerciöz et al., 2021). According to Semerciöz et al. (2021), an increase of macro algae production could shade and limit the light availability for the phytoplankton. This statement was supported based on a study done by Aldridge et al. (2021) where they found out that large-scale seaweed farming (>10,000 lines) could have a negative effect on the phytoplankton when it comes to uptake of nutrients. In this context, a deep evaluation of how phytoplankton community can be impacted due to seaweed farming is essential. Njåstad et al. (in progress) investigated and compared the nutritional state of the phytoplankton communities with farmed *S. latissima* from a cultivated site. The aim of their paper was to investigate if farmed *S. latissima* affected the phytoplankton communities when it comes to uptake of nutrients. However, the findings showed that phytoplankton were not negatively affected, but rather outcompeted *S. latissima* in uptake of nutrients.

In our results the nutritional state and biomass of the phytoplankton are in line with the findings in Njåstad et al. (in progress). The Chl *a* concentration, as a proxy for phytoplankton biomass (Cullen, 1982), showed low values in the winter when the light availability and temperature were low. When the light and temperature increased, Chl *a* increased and lead to two peaks, one in late March and one in June. This new bloom in June has also been observed in other studies (Sakshaug and Mykkestad, 1973, Haug et al., 1973). The Chl *a* concentration in the water shows high level of Chl *a* that lines with the concentrations normally found in Trønderlag waters (Etter et al., 2016). The particulate organic nitrogen, phosphorous and carbon showed almost the same pattern of variation as Chl *a*, the only difference was that the first Chl *a* peak in March was not as visible for the particulate nutrients. The values of PON, POP and POC are also agreeing with the nutritional state of the phytoplankton measured in Etter et al. (2016).

Phytoplankton have a very fast nutrient uptake capacity especially of their limiting nutrients (Olsen et al., 2014). The elemental ratios of particulate organic nutrients (PON:POC, POP:POC and PON:POP) are proxy for which nutrients that are the limiting factor for growth for the phytoplankton communities (Healey and Hendzel, 1979). In our study the POP:POC ratio was equal or slightly lower than the balance point of 15-20 $\mu\text{g P mg}^{-1}\text{ C}$, however it was in likely between the 80-100% of the balance point with suggests P-saturation and maximum growth. The N:C ratio however, showed ratios higher than the balance point of 140-160 $\mu\text{g N mg}^{-1}\text{ C}$ after the spring bloom, and way higher ratios before the spring bloom (Olsen, Yngvar. pers. comm.). This suggested that the phytoplankton was also N-saturated and had maximum growth. The N:P ratio, which reflects the limiting nutrients, showed values way higher than the balance ratio of 7.2 $\mu\text{g N } \mu\text{g}^{-1}\text{ P}$ before the spring bloom and slightly higher after the spring bloom, which suggested that there are no limiting nutrients (Redfield, 1963, Healey and Hendzel, 1979). However, the high nitrogen values measured before the spring bloom, suggested that the phytoplankton stored nitrogen (Lomas and Glibert, 2000).

Previous studies have also shown that phytoplankton are able to store phosphorus to a large extent (Ducobu et al., 1998, Lin et al., 2016). Nitrogen storage is less investigated. However, Eppley and Coatsworth (1968) found out that diatoms could store nutrients in large vacuoles. Bode et al. (1997) found out that phytoplankton were able to take up

nitrogen and assimilate it to an organic form. Other studies have also shown that diatoms can store nitrate in the vacuole in the cell (Raimbault and Mingazzini, 1987, Lomas and Glibert, 2000, Kamp et al., 2011). These observations can help explain why the N:P and N:C ratio was so high before the spring bloom, by suggesting that the phytoplankton stored nitrate and use it for growth later. The elemental ratios of N:C, P:C and N:P together with the Chl *a* content suggested that the phytoplankton had maximum growth and biomass throughout the whole experiment, and that they were not affected by the sporophyte of *S. latissima*.

4.3 Nutrient uptake and nutrient storage of *S. latissima*

S. latissima takes up inorganic nutrients from the surrounding water and uses it for growth directly or store it in internal vacuoles for later growth (Hurd et al., 2014). The sporophytes sampled and measured before the demise of the spring bloom showed the highest levels of internal nutrients (Q_N and Q_P), inorganic nutrients ($\text{NO}_3\text{-N}$ and $\text{PO}_4\text{-P}$) and Chl *a* content in February and the levels decreased until the demise of the spring bloom. The mean fraction of inorganic nitrate in the total internal nitrogen (Q_N) decreased from 13% to 0.32% from February to the demise of the spring bloom. This, shows that the sporophytes had a higher inorganic nitrate storage in the winter period (Chapman and Craigie, 1977, Jevne et al., 2020). During the summer period the fraction of inorganic nitrate was low for both the CTL and FER sporophytes, suggesting that the stored nutrients during the winter was used for growth in the spring. The mean fraction of inorganic phosphate in the total phosphorus (Q_P) did not decrease but was kept stable at $29 \pm 3.3 \%$ in the period before the spring bloom. This suggested that the sporophytes had a higher storage of inorganic phosphate in the winter period (Pedersen et al., 2010).

The N:P ratio before the spring bloom were $7.92 \pm 0.21 \mu\text{g N } \mu\text{g}^{-1} \text{P}$ and higher for the treatments measured after the spring bloom (Table 3.6). The ratio reflects the limiting nutrients that affect the growth of phytoplankton (Healey and Hendzel, 1979), but how it can be used to evaluate nutrient limitation in sporophytes are less investigated. However, the ratio measured was higher than the balance point for phytoplankton (7.2, weight) which corresponds to the Redfield ratio of molar (1:16) (Redfield, 1963, Njåstad et al., in progress). However, Atkinson and Smith (1983) calculated a ratio by examining 92 species of benthic macroalga that gave a molar N:P ratio of 30:1. The ratio of 30:1 is equivalent to a balance point around 13.6 (weight), which is close to and a slightly higher than the ratios measured in FER and Fertilized-FER sporophytes after the spring bloom. The CTL, however, had a slightly lower values suggesting that phosphorus was the limiting nutrient for the sporophyte growth.

The net uptake of both nitrogen (V_N) and phosphorus (V_P) was also higher in the early stages (February), which supported the findings in Wallentinus (1984) where young tissue has higher uptake rate than older tissue. In addition, the high net uptake can be supported by the sporophytes ability to store nutrients for later use, as discussed above (Rey, 2004). In the CTL sporophytes the net uptake rate of nitrogen (V_N) showed values below zero already in April and the net uptake of phosphorus (V_P) were low around zero in April-May and below zero in June. Net uptake close to or below zero suggested inefficient uptake of nutrients and used stored internal nutrients for growth (Njåstad et al., in progress). This is supported by the decreasing content of Q_N and Q_P in the CTL sporophytes during the spring and the low available dissolved inorganic nutrients present in the seawater basin.

4.3.1 The fertilization treatment of FER sporophytes

The Fertilized-FER sporophytes which was sampled immediately after the fertilization treatment showed internal values of $\text{NO}_3\text{-N}$ and $\text{PO}_4\text{-P}$ higher than the FER sporophytes, confirming the idea that after an enriched treatment the sporophytes would take up nutrients. The content of $\text{NO}_3\text{-N}$ and $\text{PO}_4\text{-P}$ measured the next sampling date of FER sporophytes were low and showed no significant difference from the CTL. This suggested that the FER sporophytes used the inorganic nutrients taken up in the fertilization treatment for growth or other metabolic processes immediately, or assimilated it and stored it as organic nutrients (Hurd et al., 2014). The net uptake which is based on the internal Q_N and Q_P and specific growth rate showed increasing positive values, which supports the suggestion that the sporophytes absorbed nutrients and assimilated it.

The FER sporophytes gradually increased their internal nitrogen (Q_N) content, and in June the internal nitrogen, phosphorous (Q_P) and Chl *a* content increased rapidly. The fertilization doze and incubation time increased in June, which can be the reason for the rapid increase. Even though the fertilization doze given in the beginning (April-May) was twice the concentration the *S. latissima* is exposed to in the nature (Forbord et al., 2021), the sporophytes did not increase their growth and nutrient content remarkably. The end concentration in the tank after the fertilization treatment showed that over 50 percent of the fertilization doze were not taken up by the sporophytes in the first three fertilizations, supporting other authors who found that sporophytes needed longer time to have a higher nutrient uptake (Forbord et al., 2021). When seaweed are nutrient-limited the sporophytes lag in uptake of nutrients and nutrient assimilation (Harrison and Hurd, 2001) .

4.4 Sporophyte growth and health

The growth of *S. latissima* is affected by several factors, where nutrient the key limiting factor for growth in the summer period (Hurd et al., 2014). The length in cm (Figure 3.7) for the CTL sporophytes showed a decrease in growth, the specific and the absolute growth rate did also show negative values in June. These results suggested that the outermost part of the lamina, which is the oldest part were degrading, leading to a negative growth. The degrading tissue can be caused by the decrease in intracellular nutrient content and can be reflected by the DIVING-PAM florescence measurements. The CTL sporophytes showed low values in outer most part of, and in some places no photosynthetic activity, which is a sign of unhealthy and stressed tissue. When tissue of *S. latissima* is unhealthy or degraded the tissue becomes thin and bleached (Han and Kain, 1996). As shown in the picture of the CTL sporophyte in Figure 3.11 the sporophytes lamina was bleached and thin compared to the FER sporophytes. Bleaching of the lamina is caused by loss of pigment, which can be a result of nutrient limitations (Hanisak, 1990, Forbord et al., 2021). These results are in line with the low values of Chl *a* per dry weight. Chl *a* is the most important pigment the sporophytes have because it a part of the photosynthesis. The loss of Chl *a* can have been a contributor to the bleached color (Li et al., 2020). The FER sporophytes on the other hand, had an increasing growth and a photosynthetic activity around 0.6 Fv/Fm in the inner and youngest part of the lamina, which is normal values for *S. latissima* (Heinrich et al., 2012, Hanelt, 2018, Gordillo et al., 2022).

4.5 Relationship between intracellular nutrient contents and specific growth rate

By using the Droop-model a positive correlation between the intracellular nutrients (Q_N and Q_P) and specific growth was established (Droop, 1974), which reflects the correlation found for phytoplankton (Healey and Hendzel, 1979). This supports the fact that the model can be used for macroalgae as well (Hafting, 1999, Kopczak et al., 1991, Njåstad et al., in progress). By using the Droop-model an estimation of the maximum saturation level of nutrients (Q_m) that leads to a maximum growth (μ_{max}) was made (Droop, 1974). The hyperbola curve representing from the Droop-equation (Eq. 1.1) showed that intracellular nutrient of nitrogen (Q_N) and phosphorus (Q_P) present in the young sporophytes sampled 23rd of February and 2nd of March had the maximum growth rate (μ_{max}) of $0.048 \pm 0.003 \mu \text{ day}^{-1}$. A growth rate of around 0.05 day^{-1} has been documented by Forbord et al. (2020) and Forbord et al. (2021) in N-saturated sporophytes.

The Droop-model was also used to estimate the lowest intracellular nutrient content that allowed positive specific growth (Droop, 1974). In June, the internal nutrients (Q_N and Q_P) in the CTL sporophytes showed values lower than estimated Q_0 for the *S. latissima* in this experiment. The Q_0 was estimated to be $4.5 \pm 0.42 \mu\text{g N mg}^{-1} \text{ DW}$ for nitrogen and $0.44 \pm 0.06 \mu\text{g P mg}^{-1} \text{ DW}$ for phosphorous. The mean intracellular content of nitrogen and phosphorus showed values of $3.42 \pm 0.21 \mu\text{g N mg}^{-1} \text{ DW}$ and $0.39 \pm 0.15 \mu\text{g P mg}^{-1} \text{ DW}$, which suggested that the CTL sporophyte was severe nutrient exhausted with no growth. The FER sporophytes on the other hand, showed average values higher than the estimated Q_0 . This suggested that the sporophytes had enough internal nutrients to have growth throughout the experiment.

By comparing the net uptake of nutrients (V_N and V_P) with the specific growth rate (μ), the negative and low V_N and V_P values in CTL sporophytes resulted in negative growth rates. The FER sporophytes which got fertilized showed positive net uptake of nutrients and had positive growth rate. This is also supported by the ΔQ values, when the change in nutrients is negative there is no uptake off nutrients, and vice versa. This shows that with low nutrients available in the seawater basin, the sporophytes used the internal nutrients stored before the spring bloom. When the internal nutrient content decrease to levels below the minimum nutrient content that allow growth (Q_0) the sporophytes showed negative growth, which support the degrading tissue discussed above. With low nutrient storage the sporophytes show low competitive ability to take up nutrients and by that the growth decreased.

The Q_N and Q_P content are important factors for the physiological state of the seaweed, and can differ between species, development stages, life history and nutritional status (Jevne et al., 2020). The Q_0 is dependent on the limiting nutrient, and in our case the data suggested that phosphorus was the limiting nutrient. *S. latissima* require more nitrogen than phosphorus to grow (Wang et al., 2014, Lubsch et al., 2020). By this, the sporophytes showed increasing growth even though the Q_{0P} was low, since the Q_N was the main driver for growth. In our study the sporophytes used were small and young. The sporophytes used in the other studies was larger and had different life history and it is therefore difficult to compare the data (Jevne et al., 2020, Forbord et al., 2021, Wang et al., 2014).

5 Conclusion

FAO proposed cultivation of the sea and aquaculture as the industry that could be leading in increasing the food production for the growing human population. Cultivation of seaweed is a fast-growing industry in Europe that produces sustainable products with many different purposes. To increase the production and yield in a sustainable manner, it is important to understand the fundamentals of how farmed seaweed interacts with the ecosystem, in terms of potential risks associated to the cultivation and how nutrient and light availability effects the uptake of nutrient and growth.

Results from this thesis showed no signs of nutrient limitations and maximum growth throughout the experiment of the phytoplankton communities in the basin. The CTL sporophytes that were kept undisturbed in the basin showed low competitive ability in nutrient uptake, which resulted in a decrease of internal nutrients. Values obtained were lower than the estimated Q_0 , causing impacts on growth, degraded tissue with no photosynthetic activity in some cases, and a negative net uptake. All these results suggested that that CTL sporophytes had low ability to compete with the phytoplankton in uptake of nutrients. By fertilizing *S. latissima* (FER) with high nutrient concentrations the competitive ability increased. The FER sporophytes showed the opposite trend as the CTL, with increasing internal nutrients, Chl *a*, growth, and net uptake of nutrients. This supports our hypothesis that sporophytes of *S. latissima* treated regularly with seawater enriched with nutrients after the spring bloom will show a higher intracellular nutrient content and growth rate than the sporophytes of *S. latissima* kept as unfertilized control, competing with the phytoplankton. To conclude, the results suggested that there is competition between *S. latissima* and phytoplankton when taking up nutrients, where *S. latissima* is affected negatively, and that fertilization increased the competitive ability.

References

- ABBOTT, D. W., AASEN, I. M., BEAUCHEMIN, K. A., GRONDAHL, F., GRUNINGER, R., HAYES, M., HUWS, S., KENNY, D. A., KRIZSAN, S. J. & KIRWAN, S. F. 2020. Seaweed and seaweed bioactives for mitigation of enteric methane: Challenges and opportunities. *Animals*, 10, 2432.
- ALDRIDGE, J., MOONEY, K., DABROWSKI, T. & CAPUZZO, E. 2021. Modelling effects of seaweed aquaculture on phytoplankton and mussel production. Application to Strangford Lough (Northern Ireland). *Aquaculture*, 536, 736400.
- ATKINSON, M. & SMITH, S. 1983. C: N: P ratios of benthic marine plants 1. *Limnology and Oceanography*, 28, 568-574.
- BARTSCH, I., WIENCKE, C., BISCHOF, K., BUCHHOLZ, C. M., BUCK, B. H., EGGERT, A., FEUERPFEL, P., HANELT, D., JACOBSEN, S. & KAREZ, R. 2008. The genus *Laminaria* sensu lato: recent insights and developments. *European journal of phycology*, 43, 1-86.
- BEER, S. & BJÖRK, M. 2000. Measuring rates of photosynthesis of two tropical seagrasses by pulse amplitude modulated (PAM) fluorometry. *Aquatic Botany*, 66(1), 69-76.
- BEER, S., LARSSON, C., PORYAN, O. & AXELSSON, L. 2000. Photosynthetic rates of *Ulva* (Chlorophyta) measured by pulse amplitude modulated (PAM) fluorometry. *European Journal of Phycology*, 35(1), 69-74.
- BHATIA, S., SHARMA, K., DAHIYA, R. & BERA, T. 2015. Plant tissue culture. *Modern applications of plant biotechnology in pharmaceutical sciences*, 31-107.
- BODE, A., BOTAS, J. & FERNANDEZ, E. 1997. Nitrate storage by phytoplankton in a coastal upwelling environment. *Marine Biology*, 129, 399-406.
- BOLTON, J. & LÜNING, K. 1982. Optimal growth and maximal survival temperatures of Atlantic *Laminaria* species (Phaeophyta) in culture. *Marine Biology*, 66, 89-94.
- BUCHHOLZ, C. M., KRAUSE, G. & BUCK, B. H. 2012. Seaweed and man. *Seaweed biology: Novel insights into ecophysiology, ecology and utilization*, 471-493.
- CAI, J., LOVATELLI, A., AGUILAR-MANJARREZ, J., CORNISH, L., DABBADIE, L., DESROCHERS, A., DIFFEY, S., GARRIDO GAMARRO, E., GEEHAN, J. & HURTADO, A. 2021. Seaweeds and microalgae: an overview for unlocking their potential in global aquaculture development. *FAO Fisheries and Aquaculture Circular*.
- CHAPMAN, A. & CRAIGIE, J. 1977. Seasonal growth in *Laminaria longicuris*: relations with dissolved inorganic nutrients and internal reserves of nitrogen. *Marine Biology*, 40, 197-205.
- CHAPMAN, A., MARKHAM, J. & LÜNING, K. 1978. Effects of nitrate concentration on the growth and physiology of *Laminaria saccharina* (Phaeophyta) in culture 1, 2. *Journal of phycology*, 14, 195-198.
- CULLEN, J. J. 1982. The deep chlorophyll maximum: comparing vertical profiles of chlorophyll a. *Canadian Journal of Fisheries and Aquatic Sciences*, 39, 791-803.
- DEININGER, A., BEKKBY, T., TRANNUM, H. C., BORGERSEN, G., EIKREM, W., FRIGSTAD, H., HARVEY, E. T., HEGGEM, T., MENGEOT, C. & KVILE, K. Ø. 2022. ØKOKYST-DP Norskehavet Sør, Årsrapport 2021. *NIVA-rapport*.
- DHARGALKAR, V. & PEREIRA, N. 2005. Seaweed: promising plant of the millennium.
- DILLEHAY, T. D., RAMÍREZ, C., PINO, M., COLLINS, M. B., ROSSEN, J. & PINO-NAVARRO, J. D. 2008. Monte Verde: seaweed, food, medicine, and the peopling of South America. *science*, 320, 784-786.
- DIRECTORATE OF FISHERIES. 2023. *Akvakulturstatistikk (tidserier)-Alger*. [Online]. Available: <https://www.fiskeridir.no/Akvakultur/Tall-og-analyse/Akvakulturstatistikk-tidsserier/Alger> [Accessed May 6 2023].

- DROOP, M. 1974. The nutrient status of algal cells in continuous culture. *Journal of the Marine Biological Association of the United Kingdom*, 54, 825-855.
- DUARTE, C. M., WU, J., XIAO, X., BRUHN, A. & KRAUSE-JENSEN, D. 2017. Can seaweed farming play a role in climate change mitigation and adaptation? *Frontiers in Marine Science*, 4, 100.
- DUCOBU, H., HUISMAN, J., JONKER, R. R. & MUR, L. R. 1998. Competition between a prochlorophyte and a cyanobacterium under various phosphorus regimes: comparison with the Droop model. *Journal of Phycology*, 34, 467-476.
- EPPLEY, R. W. & COATSWORTH, J. L. 1968. UPTAKE OF NITRATE AND NITRITE BY DITYLUM BRIGHTWELLII-KINETICS AND MECHANISMS 1 2. *Journal of Phycology*, 4, 151-156.
- ETTER, S., ANDRESEN, K., LEIKNES, Ø., WANG, X. & OLSEN, Y. 2016. Miljødokumentasjon Trønderlag - Utslipp og vurdering av miljøvirkninger av næringssalter tilført fra oppdrett i Trøndelag regionen i 2014. Trondhjem biologiske stasjon, Institutt for biologi. NTNU internrapport. .
- FAO 2006. State of world aquaculture. *FAO Fisheries Technical Paper*. No. 500. Rome.
- FAO 2018. The State of World Fisheries and Aquaculture 2018- Meeting the sustainable development goals. Rome.
- FAO 2020. The State of World Fisheries and Aquaculture 2020. *The State of World Fisheries and Aquaculture 2020. Sustainability in action*. Rome.
- FAO 2021. FAO Yearbook. Fishery and Aquaculture Statistics 2019/FAO annuaire. Statistiques des pêches et de l'aquaculture 2019/FAO anuario. Estadísticas de pesca y acuicultura 2019. Rome/Roma. .
- FORBORD, S., ETTER, S. A., BROCH, O. J., DAHLEN, V. R. & OLSEN, Y. 2021. Initial short-term nitrate uptake in juvenile, cultivated *Saccharina latissima* (Phaeophyceae) of variable nutritional state. *Aquatic Botany*, 168, 103306.
- FORBORD, S., STEINHOVDEN, K. B., SOLVANG, T., HANDÅ, A. & SKJERMO, J. 2020. Effect of seeding methods and hatchery periods on sea cultivation of *Saccharina latissima* (Phaeophyceae): a Norwegian case study. *Journal of Applied Phycology*, 32, 2201-2212.
- FORTES, M. & LÜNING, K. 1980. Growth rates of North Sea macroalgae in relation to temperature, irradiance and photoperiod. *Helgoländer Meeresuntersuchungen*, 34, 15-29.
- GHOSE, B. 2014. Food security and food self-sufficiency in China: from past to 2050. *Food and Energy Security*, 3, 86-95.
- GORDILLO, F. J., CARMONA, R. & JIMENEZ, C. 2022. A Warmer Arctic Compromises Winter Survival of Habitat-Forming Seaweeds. *Frontiers in Marine Science*, 8, 2020.
- HAFTING, J. T. Effect of tissue nitrogen and phosphorus quota on growth of *Porphyra yezoensis* blades in suspension cultures. Sixteenth International Seaweed Symposium: Proceedings of the Sixteenth International Seaweed Symposium held in Cebu City, Philippines, 12–17 April 1998, 1999. Springer, 305-314.
- HAN, T. & KAIN, J. M. 1996. Effect of photon irradiance and photoperiod on young sporophytes of four species of the Laminariales. *European Journal of Phycology*, 31, 233-240.
- HANCKE, K., BEKKBY, T., GILSTAD, M., CHAPMAN, A. & CHRISTIE, H. 2018. Tare dyrking-mulige miljøeffekter, synergier og konflikter med andre interesser i kystsonen.
- HANELT, D. 2018. Photosynthesis assessed by chlorophyll fluorescence. In *Bioassays* (pp. 169-198). Elsevier.
- HANISAK, M. D. 1990. The use of *Gracilaria tikvahiae* (Gracilariales, Rhodophyta) as a model system to understand the nitrogen nutrition of cultured seaweeds. *Hydrobiologia*, 204, 79-87.
- HARRISON, P. J. & HURD, C. L. 2001. Nutrient physiology of seaweeds: application of concepts to aquaculture. *Cahiers de biologie marine*, 42, 71-82.
- HAUG, A., MYKLESTAD, S. & SAKSHAUG, E. 1973. Studies on the phytoplankton ecology of the Trondheimsfjord. I. The chemical composition of phytoplankton populations. *Journal of Experimental Marine Biology and Ecology*, 11, 15-26.

- HEALEY, F. & HENDZEL, L. 1979. Indicators of phosphorus and nitrogen deficiency in five algae in culture. *Journal of the Fisheries Board of Canada*, 36, 1364-1369.
- HEGSETH, E. N. & SAKSHAUG, E. 1983. Seasonal variation in light-and temperature-dependent growth of marine planktonic diatoms in in situ dialysis cultures in the Trondheimsfjord, Norway (63° N). *Journal of Experimental Marine Biology and Ecology*, 67, 199-220.
- HEINRICH, S., VALENTIN, K., FRICKENHAUS, S., JOHN, U. & WIENCKE, C. 2012. Transcriptomic analysis of acclimation to temperature and light stress in *Saccharina latissima* (Phaeophyceae).
- HENTATI, F., TOUNSI, L., DJOMDI, D., PIERRE, G., DELATTRE, C., URSU, A. V., FENDRI, I., ABDELKAFI, S. & MICHAUD, P. 2020. Bioactive polysaccharides from seaweeds. *Molecules*, 25, 3152.
- HOWARTH, R. W. 2014. A bridge to nowhere: methane emissions and the greenhouse gas footprint of natural gas. *Energy Science & Engineering*, 2, 47-60.
- HURD, C. L., HARRISON, P. J., BISCHOF, K. & LOBBAN, C. S. 2014. *Seaweed ecology and physiology*, Cambridge University Press.
- HURD, C. L., NELSON, W. A., FALSHAW, R. & NEILL, K. F. 2004. History, current status and future of marine macroalgal research in New Zealand: Taxonomy, ecology, physiology and human uses. *Phycological Research*, 52, 80-106.
- JEVNE, L. S., FORBORD, S. & OLSEN, Y. 2020. The effect of nutrient availability and light conditions on the growth and intracellular nitrogen components of land-based cultivated *Saccharina latissima* (Phaeophyta). *Frontiers in Marine Science*, 7, 557460.
- KAMP, A., DE BEER, D., NITSCH, J. L., LAVIK, G. & STIEF, P. 2011. Diatoms respire nitrate to survive dark and anoxic conditions. *Proceedings of the National Academy of Sciences*, 108, 5649-5654.
- KOPCZAK, C. D., ZIMMERMAN, R. C. & KREMER, J. N. 1991. Variation in nitrogen physiology and growth among geographically isolated populations of the giant kelp, *Macrocystis pyrifera* (phaeophyta) 1. *Journal of Phycology*, 27, 149-158.
- KRAAN, S. 2013. Mass-cultivation of carbohydrate rich macroalgae, a possible solution for sustainable biofuel production. *Mitigation and Adaptation Strategies for Global Change*, 18, 27-46.
- KÜHL, M., GLUD, R. N., BORUM, J., ROBERTS, R., & RYSGAARD, S. 2001. Photosynthetic performance of surface-associated algae below sea ice as measured with a pulse amplitude-modulated (PAM) fluorometer and O₂ microsensors. *Marine ecology progress series*, 223, 1-14.
- KUMAR, C. S., GANESAN, P., SURESH, P. & BHASKAR, N. 2008. Seaweeds as a source of nutritionally beneficial compounds-a review. *Journal of Food Science and Technology*, 45, 1.
- LANE, C. E., MAYES, C., DRUEHL, L. D. & SAUNDERS, G. W. 2006. A multi-gene molecular investigation of the kelp (Laminariales, Phaeophyceae) supports substantial taxonomic re-organization 1. *Journal of phycology*, 42, 493-512.
- LEAN, I. J., GOLDBERGER, H. M., GRANT, T. M. & MOATE, P. J. 2021. A meta-analysis of effects of dietary seaweed on beef and dairy cattle performance and methane yield. *PLoS One*, 16, e0249053.
- LI, H., MONTEIRO, C., HEINRICH, S., BARTSCH, I., VALENTIN, K., HARMS, L., GLÖCKNER, G., CORRE, E. & BISCHOF, K. 2020. Responses of the kelp *Saccharina latissima* (Phaeophyceae) to the warming Arctic: from physiology to transcriptomics. *Physiologia plantarum*, 168, 5-26.
- LIM, J.-Y., HUI, S.-L., CHEE, S.-Y. & WONG, C.-L. 2018. *Sargassum siliculosum* J. Agardh extract as potential material for synthesis of bioplastic film. *Journal of Applied Phycology*, 30, 3285-3297.
- LIN, S., LITAKER, R. W. & SUNDA, W. G. 2016. Phosphorus physiological ecology and molecular mechanisms in marine phytoplankton. *Journal of Phycology*, 52, 10-36.
- LIU, Y. 2007. Overview of some theoretical approaches for derivation of the Monod equation. *Applied microbiology and biotechnology*, 73, 1241-1250.

- LOMAS, M. W. & GLIBERT, P. M. 2000. Comparisons of nitrate uptake, storage, and reduction in marine diatoms and flagellates. *Journal of Phycology*, 36, 903-913.
- LUBSCH, A., LANSBERGEN, R. & POELMAN, M. 2020. Seaweed factsheet: Nutrient uptake and requirements: carrying capacity in seaweed cultivation.
- MILLER, F. P. 2008. After 10,000 years of agriculture, whither agronomy? *Agronomy Journal*, 100, 22-34.
- MOY, F. E. & CHRISTIE, H. 2012. Large-scale shift from sugar kelp (*Saccharina latissima*) to ephemeral algae along the south and west coast of Norway. *Marine Biology Research*, 8, 309-321.
- NALDI, M. & VIAROLI, P. 2002. Nitrate uptake and storage in the seaweed *Ulva rigida* C. Agardh in relation to nitrate availability and thallus nitrate content in a eutrophic coastal lagoon (Sacca di Goro, Po River Delta, Italy). *Journal of Experimental Marine Biology and Ecology*, 269, 65-83.
- NETO, R. T., MARÇAL, C., QUEIROS, A. S., ABREU, H., SILVA, A. M. & CARDOSO, S. M. 2018. Screening of *Ulva rigida*, *Gracilaria* sp., *Fucus vesiculosus* and *Saccharina latissima* as Functional Ingredients. *International Journal of Molecular Sciences*, 19, 2987.
- NIELSEN, M. M., MANNS, D., D'ESTE, M., KRAUSE-JENSEN, D., RASMUSSEN, M. B., LARSEN, M. M., ALVARADO-MORALES, M., ANGELIDAKI, I. & BRUHN, A. 2016. Variation in biochemical composition of *Saccharina latissima* and *Laminaria digitata* along an estuarine salinity gradient in inner Danish waters. *Algal research*, 13, 235-245.
- NJÅSTAD, E., NEVES, L., SKROVE, T. & OLSEN, Y. in progress. Nutrient competition and environmental interaction of farmed *Saccharina latissima* (Phaeophyta) and phytoplankton communities.
- O'CONNOR, K. 2017. *Seaweed: a global history*, Reaktion Books.
- OLSEN, Y. 2011. Resources for fish feed in future mariculture. *Aquaculture Environment Interactions*, 1, 187-200.
- OLSEN, Y., REINERTSEN, H., SOMMER, U. & VADSTEIN, O. 2014. Responses of biological and chemical components in North East Atlantic coastal water to experimental nitrogen and phosphorus addition—A full scale ecosystem study and its relevance for management. *Science of the total environment*, 473, 262-274.
- PEDERSEN, M. F., BORUM, J. & FOTEL, F. L. 2010. Phosphorus dynamics and limitation of fast-and slow-growing temperate seaweeds in Oslofjord, Norway. *Marine Ecology Progress Series*, 399, 103-115.
- RAIMBAULT, P. & MINGAZZINI, M. 1987. Diurnal variations of intracellular nitrate storage by marine diatoms: effects of nutritional state. *Journal of experimental marine biology and ecology*, 112, 217-232.
- REDFIELD, A. C. 1963. The influence of organisms on the composition of seawater. *The sea*, 2, 26-77.
- REY, F. 2004. Phytoplankton: the grass of the sea. In: SKJOLDAL, H. R. (ed.) *The Norwegian Sea Ecosystem*. Trondheim: Tapir Academic Press.
- SAKSHAUG, E. & MYKLESTAD, S. 1973. Studies on the phytoplankton ecology of the Trondheimsfjord. III. Dynamics of phytoplankton blooms in relation to environmental factors, bioassay experiments and parameters for the physiological state of the populations. *Journal of Experimental Marine Biology and Ecology*, 11, 157-188.
- SARMIENTO, J. L. & GRUBER, N. 2006. *Ocean Biogeochemical Dynamics* Princeton University Press.
- SEMERCIOZ, A. S., SOYALP, K., ULU, G. & ÖZILGEN, M. 2021. Effects of energy storage by the seaweeds on their ecosystem. *Energy Storage*, 3, e266.
- SJØTUN, K. 1993. Seasonal lamina growth in two age groups of *Laminaria saccharina* (L.) Lamour. in western Norway.
- SKJERMO, J., AASEN, I. M., ARFF, J., BROCH, O. J., CARVAJAL, A. K., CHRISTIE, H. C., FORBORD, S., OLSEN, Y., REITAN, K. I. & RUSTAD, T. 2014. A new Norwegian bioeconomy based on cultivation and processing of seaweeds: Opportunities and R&D needs.

- SLEGGERS, P. M., HELMES, R. J. K., DRAISMA, M., BROEKEMA, R., VLOTTES, M. & VAN DEN BURG, S. W. K. 2021. Environmental impact and nutritional value of food products using the seaweed *Saccharina latissima*. *Journal of Cleaner Production*, 319, 128689.
- STÉVANT, P., REBOURS, C. & CHAPMAN, A. 2017. Seaweed aquaculture in Norway: recent industrial developments and future perspectives. *Aquaculture International*, 25, 1373-1390.
- UN. 2019. *United Nation: World Population Prospects: The 2019 Revision Population Database* [Online]. <https://population.un.org/wpp/>. [Accessed 03.11 2022].
- VAN DEN BURG, S., DAGEVOS, H. & HELMES, R. 2021. Towards sustainable European seaweed value chains: a triple P perspective. *ICES Journal of Marine Science*, 78, 443-450.
- VAN DEN HOEK, C. & DONZE, M. 1967. Algal phytogeography of the European Atlantic coasts. *Blumea: Biodiversity, Evolution and Biogeography of Plants*, 15, 63-89.
- VISCH, W., RAD-MENÉNDEZ, C., NYLUND, G. M., PAVIA, H., RYAN, M. J. & DAY, J. 2019. Underpinning the development of seaweed biotechnology: cryopreservation of brown algae (*Saccharina latissima*) gametophytes. *Biopreservation and biobanking*, 17, 378-386.
- WALLENTINUS, I. 1984. Comparisons of nutrient uptake rates for Baltic macroalgae with different thallus morphologies. *Marine Biology*, 80, 215-225.
- WANG, X., BROCH, O. J., FORBORD, S., HANDÅ, A., SKJERMO, J., REITAN, K. I., VADSTEIN, O. & OLSEN, Y. 2014. Assimilation of inorganic nutrients from salmon (*Salmo salar*) farming by the macroalgae (*Saccharina latissima*) in an exposed coastal environment: implications for integrated multi-trophic aquaculture. *Journal of applied phycology*, 26, 1869-1878.
- WHITE, N. & MARSHALL, C. 2007. *Saccharina latissima*. Sugar kelp.
- WOOD, G. A. 1982. Data smoothing and differentiation procedures in biomechanics. *Exercise and sport sciences reviews*, 10, 308-362.
- YTRESTØYL, T., AAS, T. S. & ÅSGÅRD, T. 2015. Utilisation of feed resources in production of Atlantic salmon (*Salmo salar*) in Norway. *Aquaculture*, 448, 365-374.



Norwegian University of
Science and Technology